

**DEVELOPMENT OF HYPER-BRANCHED
POLYLACTIDE AND PREPARATION OF
SILICA/POLYLACTIDE BIOCOMPOSITES FOR USE IN
PACKAGING APPLICATION**

BY

NARISARA JAIKAEW

**A THESIS SUBMITTED IN PARTIAL FULFILLMENT OF THE
REQUIREMENTS FOR THE DEGREE OF MASTER OF SCIENCE
(ENGINEERING AND TECHNOLOGY)
SIRINDHORN INTERNATIONAL INSTITUTE OF TECHNOLOGY
THAMMASAT UNIVERSITY
ACADEMIC YEAR 2015**

**DEVELOPMENT OF HYPER-BRANCHED
POLYLACTIDE AND PREPARATION OF
SILICA/POLYLACTIDE BIOCOMPOSITES FOR USE IN
PACKAGING APPLICATION**

BY

NARISARA JAIKAEW

**A THESIS SUBMITTED IN PARTIAL FULFILLMENT OF THE
REQUIREMENTS FOR THE DEGREE OF MASTER OF SCIENCE
(ENGINEERING AND TECHNOLOGY)**

SIRINDHORN INTERNATIONAL INSTITUTE OF TECHNOLOGY

THAMMASAT UNIVERSITY

ACADEMIC YEAR 2015



DEVELOPMENT OF HYPER-BRANCHED POLYLACTIDE AND
PREPARATION OF SILICA/POLYLACTIDE BIOCOMPOSITES FOR USE IN
PACKAGING APPLICATION

A Thesis Presented

By

NARISARA JAIKAEW

Submitted to

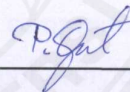
Sirindhorn International Institute of Technology

Thammasat University

In partial fulfillment of the requirements for the degree of
MASTER OF SCIENCE (ENGINEERING AND TECHNOLOGY)

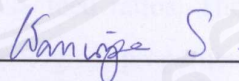
Approved as to style and content by

Advisor and Chairperson of Thesis Committee



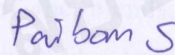
(Assoc. Prof. Dr. Pakorn Opaprakasit, Ph.D.)

Committee Member and
Chairperson of Examination Committee



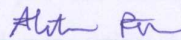
(Asst. Prof. Dr. Wanwipa Siriwatwechakul, Ph.D.)

Committee Member



(Asst. Prof. Dr. Paiboon Sreearunothai, Ph.D.)

Committee Member



(Dr. Atitsa Petchsuk, Ph.D.)

May 2016

Abstract

DEVELOPMENT OF HYPER-BRANCHED POLYLACTIDE AND PREPARATION OF SILICA/POLYLACTIDE BIOCOMPOSITES FOR USE IN PACKAGING APPLICATION

by

NARISARA JAIKAEW

Master of Science (Engineering and Technology) Sirindhorn International Institute of
Technology Thammasat University, 2015

This study is aimed to develop biocomposite materials from hyperbranched polylactide copolymers. The thesis is divided into two parts. The first part focuses on synthesis and characterization of hyper-branched poly (L-lactide) (*hbPLLAs*), and linear poly (L-lactide) (*l-PLLA*), and *l-PLLA/hbPLLAs* blended films. The second part is concentrated on the development of *l-PLLA/silica* composites. *hbPLLAs* are synthesized by copolymerization of *l*-lactide (LLA) using poly(ethylene imine) (PEI) as a macro-initiator. Effect of arm's lengths on structures and properties of the copolymers are investigated by varying the PEI: LLA feed ratios. The synthesized products, which show interesting mechanical and rheological properties, are used in the properties modification of commercial *l-PLLA* resin by a melt blending process. Thermal, mechanical, and rheological properties of the blends, as a function of *hbPLLAs* structures and compositions, are examined. All blend samples exhibit lower glass transition temperature (T_g), crystalline melting temperature (T_m), and complex viscosity than those of *l-PLLA* resin, which can provide many advantages in processing of the materials. In term of mechanical properties, *l-PLLA/hbPLLAs* blended with long-branched structures (i.e. *hbPLLA100*) show an increased in the modulus with an increase of *hbPLLA100* compositions. The blends properties can also be further optimized for specific applications by varying the branched structured compositions.

In the second part, a preparation process for silica particles from rich husk ash (RHA) is developed and use as a filler in a preparation of *l*-PLLA/silica biocomposite films, in order to modify their mechanical property and gas permeability, for use as packaging materials. The silica materials are produced from a simple alkali extraction process of RHA, in which PLA-*grafted*-chitosan (PCT) copolymer is employed as a polymeric surfactant. PCT are synthesized by condensation polymerization of lactic acid with chitosan oligomer at 140 °C. In the preparation of silica particles, PCT act as a surfactant for the formation of silica particles and also as a coating material which enhanced compatibility between the silica particles and *l*-PLLA matrix when they are employed in the preparation of composite materials. The *l*-PLLA/PCT-coated silica composites films show significant improvement in tensile modulus at 1.5% wt of PCT-coated silica contents. The gas permeability and selectivity of the composite films are enhanced in *l*-PLLA/PCT-coated silica composites films, which make the material a good candidate for packaging application.

Keywords: Packaging, Polylactide, Hyper-branched polymer, Copolymer, Composites, Silica particles

Acknowledgements

This thesis is a part of my study to obtain my master degree. There are many people I met during this time who had extended their support. It is a pleasant aspect that I have now the opportunity to express my heartfelt gratitude to all of you.

I would like to appreciate Assoc. Prof. Pakorn opaprakasit, my project advisor for his ideas, support, and also the valuable guidance throughout my master life. Thank you for the experience to communicate my work to the audience by giving me the opportunity to participate in many conferences and activities. Many activities those I have done with my advisor and our lab members make me feel comforted, all members here are like my family.

I also appreciate my thesis committee, Asst. Prof. Dr. Wanwipa Siritwatwechakul and Asst. Prof. Dr. Paiboon Sreearunothai, for nice discussions (during my proposal and progress exams). All suggestions help improving the quality of my work and also enhancing me to be more professional in my field.

In addition, I would like to thank all of my collaborators for the valuable inputs in my research. Thank you Dr. Atitsa Petchsuk from National Metal and Materials Technology Center (MTEC), I appreciate for all support either by words of encouragement or valuable advice. I have learnt many laboratory skills for being a good researcher. I must thank Miss Wilairut supmak, my senior in our laboratory group, for all supports in materials, information, and laboratory skills.

I would like to acknowledge the funding source and scholarship from Sirindhorn International Institute of Technology. Thank for a good environment in the campus, all SIIT members, and my class mates.

Thanks to my family and friends who have always been there for me. Thank you for your constant supports and encouragements in everything.

Table of Contents

Chapter	Title	Page
	Signature Page	i
	Acknowledgements	ii
	Abstract	iii
	Table of Contents	iv
	List of Tables	viii
	List of Figures	ix
1	Introduction	1
	1.1 Concept and significant	1
	1.2 Objectives of the study	3
	1.3 Scope of study	3
2	Literature Review	5
	2.1 Polylactide (PLA)	5
	2.2 PLA modification	7
	2.2.1 Copolymer of PLA	7
	2.2.2 Hyper-branched PLA	9
	2.2.2.1 Synthesis of hyperbranched PLA	12
	2.2.3 PLA blending	13
	2.2.4 PLA Composites	
	2.2.4.1 PLA/clays nanocomposites	15
	2.2.5 PLA/silica composites	16
3	Methodology	17
	3.1 <u>Part 1</u> Synthesis and characterization of hyper-branched PLLA (<i>hbPLLAs</i>) and <i>l</i> -PLLA/ <i>hbPLLAs</i> blended.	17
	3.1.1 Materials	17
	3.1.2 Synthesis of <i>hbPLLAs</i>	17

3.1.3	Preparation of <i>l</i> -PLLA/ <i>hb</i> PLLAs blended	18
3.1.4	Characterizations of <i>hb</i> PLLAs and <i>l</i> -PLLA/ <i>hb</i> PLLAs blends films	
3.1.4.1	Nuclear Magnetic Resonance (NMR) spectrometer	18
3.1.4.2	Differential Scanning Calorimeter (DSC)	18
3.1.4.3	Universal Testing Machine (UTM)	19
3.1.4.4	Rheometer	19
3.2	<u>Part 2</u> Preparation and characterization of PCT-coated silica particles and <i>l</i> -PLLA/ PCT coated silica composite films	20
3.2.1	Materials	20
3.2.2	Preparation of silica and PCT-coated silica	20
3.2.3	Preparation of <i>l</i> -PLLA/PCT-coated silica and <i>l</i> -PLLA/ clays composite films	21
3.2.4	Characterization of PCT-coated silica and <i>l</i> -PLLA/ PCT-coated silica composite films	21
3.2.4.1	Fourier Transform Infrared (FTIR) spectroscope	21
3.2.4.2	Scanning Electron Microscope (SEM)	21
3.2.4.3	Nitrogen gas sorption technique	21
3.2.4.4	Atomic Pycnometer	21
3.2.4.5	Universal Testing Machine (UTM)	22
3.2.4.6	Gas permeability analyzer	22
4	Results and Discussion	23
4.1	<u>Part 1</u> Synthesis and characterization of hyper-branched PLLA (<i>hb</i> PLLAs) and <i>l</i> -PLLA/ <i>hb</i> PLLAs blended.	23
4.1.1	Chemical structure of <i>hb</i> PLLAs (NMR)	23
4.1.2	Thermal property (DSC)	26
4.1.3	Mechanical property (UTM)	31

4.1.4 Rheology	34
4.2 <u>Part 2</u> Preparation and characterization of PCT-coated silica particles and <i>l</i> -PLLA/PCT-coated silica films	40
4.2.1 Chemical structure (FTIR)	40
4.2.2 Morphology (SEM)	41
4.2.3 Particles size distribution	42
4.2.4 Mechanical property (UTM)	43
4.2.5 Gas permeability	47
5 Conclusions and Recommendation	49
5.1 Conclusions	49
5.2 Recommendations	49
References	50
Appendices	
Appendix A ¹ H-NMR spectra	
Appendix B Publications	

List of Tables

Tables	Page
2.1 Properties of PLA (Material datasheet by Biomer L9000)	6
3.1 Summary on the synthesized <i>hb</i> PLLAs products	18
4.1 Results on average LLA lengths and PLLA/PEI molar ratio in <i>hb</i> PLLAs chain	23
4.2 Thermal properties of <i>l</i> -PLLA/ <i>hb</i> PLLA10 blends	30
4.3 Thermal properties of <i>l</i> -PLLA/ <i>hb</i> PLLA20 blends	30
4.4 Thermal properties of <i>l</i> -PLLA/ <i>hb</i> PLLA100 blends	31
4.5 Particle size and size distribution, surface area, and density of silica and PCT-coated silica particles	43
4.6 Tensile results of <i>l</i> -PLLA and <i>l</i> -PLLA/PCT-coated silica composite films containing particles with different sizes and blend contents	45
4.7 OTR, CO ₂ TR, and WVTR of <i>l</i> -PLLA and <i>l</i> -PLLA/PCT-coated silica composite films	46

List of Figures

Figures		Page
2.1	Chemical structures of d,d-lactide (m.p. 97°C), l,l-lactide (m.p. 97°C) and d,l-lactide (meso-lactide, m.p. 52°C).	5
2.2	Graft copolymerization of PLA onto chitosan oligomer and chemical structure of the resulting graft copolymers	9
2.3	Tan δ values as a function of CE concentration at a frequency of 1rad/s for branched-extruded aPLA and cPLA samples	10
2.4	Temperature dependence of complex viscosity (η^*) (a), storage moduli (G') (b) and loss moduli (G'') and (c) of stereocomplex blends containing different mbPDLAs	11
2.5	Scheme represents the synthesis of multiarm star copolymers PEI- <i>b</i> -PDLLA and PEI- <i>b</i> -PLLA	13
4.1	¹ H-NMR spectra and chemical structures of <i>hb</i> PLLA10 and PEI	24
4.2	DSC thermogram (2 nd heating scan) of (a) <i>hb</i> PLLA10, (b) <i>hb</i> PLLA20 and (c) <i>hb</i> PLLA100 samples	26
4.3	DSC thermograms (2 nd heating scan) of (a) <i>hb</i> PLLA10 and <i>l</i> -PLLA/ <i>hb</i> PLLA10 blends at various compositions % wt: (b) 80/20, (c) 85/15, (d) 90/10, (e) 95/5, and (f) <i>l</i> -PLLA	27
4.4	DSC thermograms (2 nd heating scan) of (a) <i>hb</i> PLLA20 and <i>l</i> -PLLA/ <i>hb</i> PLLA20 blends at various compositions % wt: (b) 80/20, (c) 85/15, (d) 90/10, (e) 95/5, and (f) <i>l</i> -PLLA	28
4.5	DSC thermograms (2 nd heating scan) of (a) <i>hb</i> PLLA100 and <i>l</i> -PLLA/ <i>hb</i> PLLA100 blends at various compositions % wt: (b) 80/20, (c) 85/15, (d) 90/10, (e) 95/5 and (f) <i>l</i> -PLLA	29
4.6	Tensile strength (a), Elongation at break (b) and Modulus (c) of <i>hb</i> PLLAs and <i>l</i> -PLLA/ <i>hb</i> PLLAs blends films, as a function of the blend composition	33
4.7	Complex viscosity, as a function of shear rate of (a) <i>l</i> -PLLA/ <i>hb</i> PLLAs blends containing different <i>hb</i> PLLAs, at a 90/10 composition and	35

	(b) <i>l</i> -PLLA/ <i>hb</i> PLLA20 blends (at a various blend compositions)	
4.8	Viscoelastic characteristics in terms of (a) complex viscosity (η^*), (b) storage modulus (G') and (c) loss modulus (G'') as a function of temperature of <i>l</i> -PLLA/ <i>hb</i> PLLAs blends at a 90/10 composition	37
4.9	Viscoelastic characteristics in terms of (a) complex viscosity (η^*), (b) storage modulus (G'), and (c) loss modulus (G'') as a function of temperature of <i>l</i> -PLLA/ <i>hb</i> PLLA20 blends (at a various blends composition)	39
4.10	FTIR spectra of silica (a) and PCT-coated silica (b) particles, and the difference spectrum (c)	41
4.11	Scanning electron microscope of silica (a) and PCT-coated silica particles (b)	42
4.12	Stress-strain behaviors of <i>l</i> -PLLA and composite containing <i>l</i> -PLLA/PCT-coated silica particles at 1.0 %wt. content.	43
4.13	Tensile properties of <i>l</i> -PLLA/PCT-coated silica composites films with different PCT-coated silica particle sizes and contents (a) Tensile strength and (b) Elongation at break	46

Chapter 1

Introduction

1.1 Concept and Significant

Degradable polyesters, whose major advantages being biocompatibility and degradability, are a group of materials of interest in biomedical, pharmaceutical, and environmental applications for replacing traditional non-degradable polymers [1, 2]. These materials are thermoplastic polymers consisting of hydrolysable linkages in their backbone [3]. Among these, polylactide or poly(lactic acid) (PLA), which is classified as thermoplastic aliphatic polyester, is one of the most attractive materials, due to its degradability, good plasticity, suitable processability, high mechanical strength, relatively low cost of production, and renewability [4, 5]. PLA can be synthesized by either polycondensation of lactic acid, or ring-opening polymerization (ROP) of lactide, dimer which is the latter is the most effective process to obtain high molecular weight PLA. However, the polymer exhibits poor thermal stability and low melts strength. This limits its use in several ways [2, 6-8]. Recently, many attempts have been made to improve PLA's properties, such as copolymerization, blending with other polymers or plasticizers, toughening by rubber materials, introduction of branched structures, stereo-complex, and nano-composites reinforcement [1, 9].

The introduction of branched structures into PLA is proven as a promising way to improve its properties [2]. Branch-structured polymers, at the same molecular weight, have lower solution and melt viscosity than its linear-structured counterparts. An addition of these materials leads to improvements in physio-chemical properties of the matrix [2, 10]. Dendrimic, and hyper-branched polymers are macromolecules containing a center core and multi branches. These groups of materials have received most attention, due to their unique properties of low viscosity and a high degree of surface functionality, which can be further designed and controlled. In addition, one of the major advantages of hyper-branched polymers is that they can be synthesized in a one-step process [11]. Petchsuk et al. [12] reported the lowering in complex viscosity of multi-branched poly(D-lactide)s (*mbPDLAs*) prepared from copolymerization of polyglycedol (PG) macroinitiator and D-lactide via the ROP

process. Various highly-branched polymers, such as polyethylene glycol (PEG), polyglycerol (PG) and polyethyleneimine (PEI) have been used as a core in the preparation of hyperbranched polylactide, due to the high reactivity of functionalized end-groups, i.e., as hydroxyl and amine [13].

Another interesting process to modify the properties of PLA is preparing it with inorganic fillers [14, 15]. Polymer composites are defined as polymer system interactions with particles to produce materials with enhanced properties. Composites of PLA with other biodegradable/biocompatible materials have been prepared for modifying thermal and mechanical properties with retain in biocompatibility and degradability [16-18]. Many inorganic types of filler have been used for preparing polymeric composite materials [19, 20]. Among these, silica (SiO_2) is one of the most popular, due to its low cost and abundant in nature [21]. There are many sources of silica such as sand, clay and ash.

Rice husk ash (RHA), which is by-product from agricultural resources, is commonly used as a major sources of silica as this contains almost 95% SiO_2 [22]. The properties of silica particle such as surface morphology, porosity and particle size can be optimized during their production processes by varying the preparation conditions. Preparing of silica particles by using precursors in the presence of different types of media, e.g., poly (ethylene glycol), or sodium dodecyl sulphate surfactants and alcohol or alcohol-based mixed solvents, can be conducted for optimizing the properties of the particles [23]. In addition, the surface modification of silica particles is required in order to achieve good enhancement characteristics by improving the compatibility between the particles and polymer matrix, especially PLLA.

1.2 Objectives of the study

The objective of this study is to enhance the properties of *l*-PLLA resin, in term of mechanical properties improvements. The enhancements are focusing on two approaches, which are an introduction of branched structures and preparation of biocomposites consisting of surface-coated silica particles.

1.3 Scope of the study

Part 1 Synthesis and characterization of hyper-branched PLLA (*hb*PLLAs) and *l*-PLLA/ *hb*PLLAs blended. The scopes of this part include;

1. Synthesis of hyper-branched PEI/PLLA copolymer (*hb*PLLAs) with different branched structure by varying the feed ratio of PEI:LA.
2. Determination of chemical structures and thermal property of the *hb*PLLAs by Nuclear Magnetic Resonance (NMR) spectrometry and Differential Scanning Calorimetric (DSC).
3. Preparation and characterizations of *hb*PLLAs and *l*-PLLA/*hb*PLLAs blended films by mixing in an internal mixer and processing by hot-press compression molding.
4. Characterization of thermal, mechanical, and rheological properties of *hb*PLLAs and *l*-PLLA/*hb*PLLAs blended films by Differential Scanning Calorimetric (DSC), Tensile and Rheological tests.

Part 2 Preparation and characterization of PCT-coated silica particles and *l*-PLLA/ PCT-coated silica films

1. Synthesis and characterization of poly (lactic acid-*grafted*-chitosan) (PCT) copolymers by condensation polymerization.
2. Preparation of PCT-coated silica particles from rich husk ash (RHA) by a sol-gel method.
3. Determination of chemical structures and interactions between silica particles and poly (lactic acid-*grafted*-chitosan) copolymer (PCT) by Fourier Transform Infrared (FTIR) spectroscopy.

4. Characterization of morphology, particle size, and surface properties of PCT-coated silica particles by Scanning Electron Microscope (SEM) and Nitrogen gas sorption techniques.
5. Preparation of *l*-PLLA/PCT-coated silica composite films by mixing in an internal mixer and a hot-press compression molding technique.
6. Characterization of mechanical and gas permeation properties of *l*-PLLA/PCT-coated silica by tensile tests and gas permeability test.

Chapter 2

Literature Review

2.1 Synthesis and properties of polylactide (PLA)

Polylactide (PLA) is produced from lactic acid monomer (LA), which is obtained from the fermentation of substrates, such as sugar cane, corn, and starch. The material is linear aliphatic polyester that has a chiral center in the molecule, leading to two optical isomers. Alternatively, PLA can be synthesized from its lactide dimer. In this regard, lactide contain 2 chiral center in its ring structure. The d,d-lactide (d-LA) and l,l-lactide (l-LA) are the optical isomer of lactide that leads to the different optical isomer structures of poly(L-lactic acid) PLLA and poly (D-lactic acid) PDLA [4, 24]. An enantiomer mixture of PLLA and PDLA can form a stererocomplex, which enhanced crystalline properties, resulting in the increase in the melting temperature (T_m) about 50°C , compared to neat linear PLA [25, 26]. The most effective way to synthesize high molecular weight PLA is a ring opening polymerization (ROP) of lactide. In the ROP process, lactic acid has to convert into the ring structure by dehydration reaction to yield lactide dimer. The dimer is then polymerized in the presence of heat and catalyst to obtain high molecular weight PLA [4, 27, 28]. The Chemical structures of d,d-lactide, l,l-lactide and d,l-lactide, and the ROP reaction are shown in Figure 2.1.

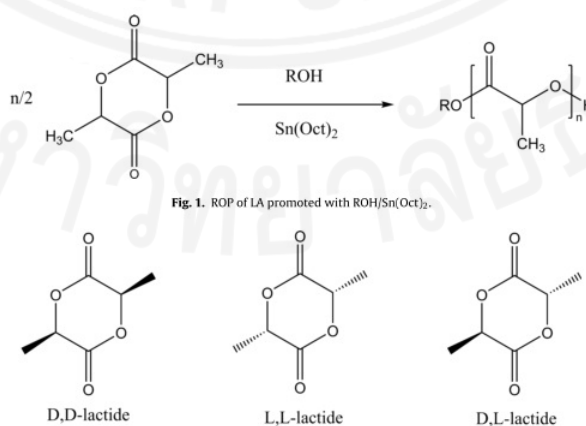


Fig. 1. ROP of LA promoted with ROH/Sn(Oct)₂.

Figure 2.1 Chemical structures of d,d-lactide (m.p. 97°C), l,l-lactide (m.p. 97°C) and d,l-lactide (meso-lactide, m.p. 52°C). m.p. = melting point.

From their molecular structure and the ability to form specific interaction into polar molecules force, PLA arrange themselves in a semi-crystalline structure. PLA has a glass transition temperature (T_g) around 55 to 59°C and a melting point at 174-184 °C [1]. The polymer shows good mechanical properties when comparable to other commercial plastics such as poly (ethylene) (PE), poly(propylene) (PP), poly(styrene) PS and poly(ethylene terephthalate) (PET) [29]. Tensile modulus of PLA is around 3 GPa, a tensile strength between 50 and 70 MPa, with an elongation at break at around 2.4%, and an impact strength close to 1.65 J/cm². The relatively high value of Young's modulus of PLA makes it an attractive choice for use as short-time packaging materials. The physical, mechanical and thermal properties of PLA are summarized in Table 2.1.

Table 2.1 Properties of PLA (Material datasheet by Biomer L9000)

Physical Properties	Metric
Density	1.25 g/cc
Moisture Absorption at Equilibrium	0.30 %
Linear Mold Shrinkage	0.0012 cm/cm
Melt Flow	3.0 - 6.0 g/10 min
Deformation	2.8 %
Mechanical Properties	Metric
Tensile Strength, Ultimate	70.0 MPa
Elongation at Break	2.4 %
Modulus of Elasticity	3.60 GPa
Flexural Strength	98.0 MPa
Charpy Impact Unnotched	1.65 J/cm ²
Charpy Impact, Notched	0.330 J/cm ²
Thermal Properties	Metric
Maximum Service Temperature, Air	50.0 °C
Vicat Softening Point	56.0 °C
Minimum Service Temperature, Air	-10.0 °C
Glass Transition Temp, T_g	55.0 °C

However, PLA is a brittle material similar to PS. The material has low impact strength and low barrier property from their amorphous domains. This leads to limitations of its in several applications [6, 7].

2.2 Modifications of PLA

2.2.1 Copolymers of PLA

PLA has attracted much attention for use in many fields because of its biodegradable and biocompatible properties. However, PLA have some disadvantages such as high brittleness, poor melt strength, low heat deflection temperature (HDT), and low thermal stability, which limit its use in their large-scale applications. Recently, many attempts have been made to improve properties of PLA, such as copolymer, blending with other polymer or plasticizer, toughening by natural rubber, and nano compositing with other polymer reinforcement. One of the interesting strategies to overcome these limitations is to prepare copolymers of PLA. In the last decade, copolymerization of lactic acid (or lactide) with hydroxyl acids, amino acids, and polymers such as polyethylene glycol (PEG) and polyethylene imine (PEI) have been conducted to improve strength, toughness, hydrophilicity, and controlled degradable properties of PLA [5, 7, 27, 30, 31]. Many research works about PLA copolymers have been studied for potential use as additives and compatibilizers for many applications, especially packaging and biomedical applications. Copolymerization of PLA creates new copolymers with different macromolecular architectures (linear, branch and star), leading to different and interesting properties, compared to typical linear PLA. PLA copolymers can be synthesized by several polymerization techniques, including polycondensation, anionic, cationic, and coordination-insertion ring-opening polymerizations.

Thai Hien Nguyen et al. successfully prepared tri-block copolymers of PLLA/PEG/PLLA. The copolymerization of PLA and PEG was conducted by ROP at 130 °C, using stannous octoate, Sn(Oct)₂, catalyst. The synthesized products were then reacted with hexamethylene diisocyanate (HDMI), a chain extending agent, to form a multi-block copolymer. The results indicated that high molecular weight triblock copolymers were obtained from a molar feed ratio of *l*-lactide OH of 98/2. The molecular weight of the products can be further increased by reacting with HDMI. The block copolymers show an increased in T_g and decreased in T_m , compared to the commercial *l*-PLLA, which provided advantages in terms of wider range of service temperatures.

M. Opaprakasit et al. studied the synthesis of PET-co-PLA copolymers by employing polycondensation of mixtures of lactic acid (LA), ethylene glycol (EG) and dimethyl terephthalate (DMT), with stannous octoate, Sn(Oct)₂ catalyst. The synthesized products were then reacted with HDMI to increase their chain lengths. The products were used to blend with commercial *l*-PLLA in order to modify their mechanical, thermal, and physical properties. The blended products showed lower brittleness than the commercial *l*-PLLA, with lower T_g. In addition, the blended products processed higher T_m and greater thermal stability than commercial *l*-PLLA, as results from the inclusion of aromatic terephthalate units in the chain structure.

In addition, the copolymers of PLA with natural polymers have also been studied. C. Thammawong et al., successfully synthesized Polylactia acid-*grafted*-Chitosan copolymers by polycondensation of lactic acid (LA) with Chitosan oligomer and employed as stabilizers for magnetic nanoparticles preparation in water medium for use in the preparation of Naproxen (NPX) drug-loaded magnetic nanoparticles (MNPs). It was found that the amine groups in Chitosan were grafted with hydroxyl groups of PLA. The copolymer was prepared by heating LA 100 mL at 120 °C for 1 hour and then increased to 140 °C for 1 hour. Chitosan (wt% of LA) and SnCl₂ catalyst (0.2 mol % of LA) were subsequently added. The polymerization was kept at 140°C for 3 hours and a high vacuum pump was then applied for 1 hour to remove monomer residue and by-products. Chemical structure of the resulting graft copolymers are shown in Figure 2.2 [32].

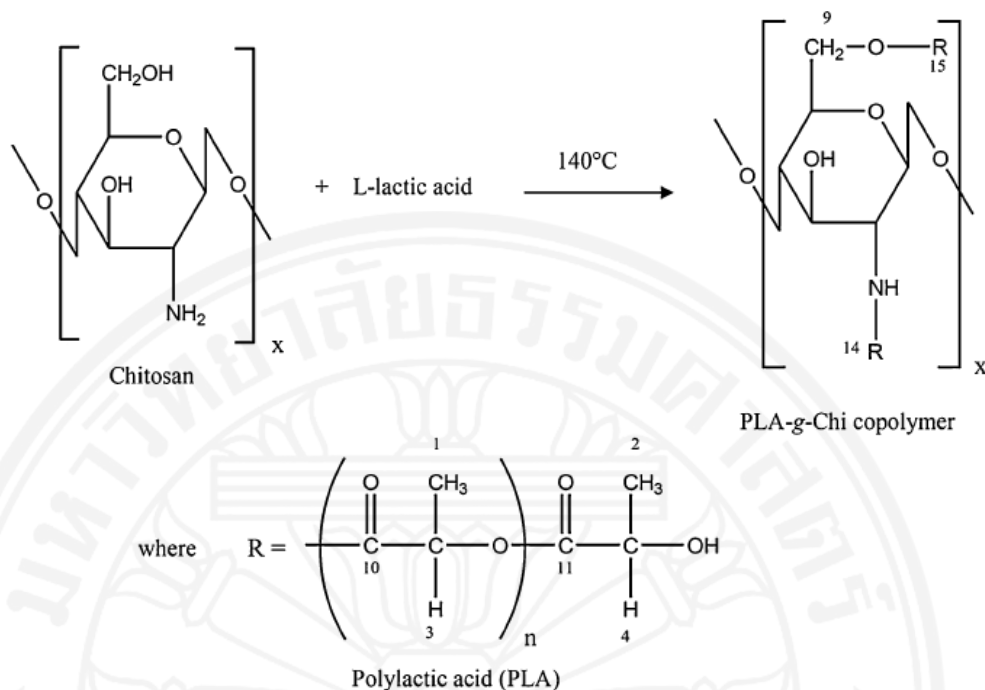


Figure 2.2 Graft copolymerization of PLA onto chitosan oligomer and chemical structure of the resulting graft copolymers.

2.2.2 Hyper-branched PLA

Branched polymers have different physiochemical properties, compared to their linear structured counterparts [11]. During the melt processing polymer, to poor melt stability may lead to chain scission due to hydrolysis and also thermal instability [33]. The degree of damage is further increase when the processing is conducted at higher temperatures. Linear PLA exhibits low melt strength that limits it to certain applications. The introduction of chain branching agents is an effective way to improve the melt strength of PLA. With the introduction of branching, the rheological properties of PLA can be significantly modified [2]. Many researchers have been reported the unique properties of branched polymers such as good melt strength, good solubility, and multi-functionality [2, 11]. Mihai et al. reported an increase in shear viscosity and melt elasticity of branched PLLA by using a multifunctional styrene-acrylic epoxy copolymers as chain extenders [34]. The ratio of viscous to elasticity behaviors at a given oscillation frequency ($\tan \delta$) of the extruded PLA (0% Chain extender (CE)) was about 20 and decreased continuously to a value around 4 with increasing CE concentration from 0 to 2%. The decrease in $\tan \delta$ value also indicates

an increase of melt elasticity. This is a result from the increase in the polymer branches, when the CE contents increased the number of entanglements between PLLA macromolecular chains. $\text{Tan } \delta$ values of aPLA (PLA8302D amorphous grade) and cPLA (PLA4023D semi-crystalline grade) measured at 180°C as a function of the CE contents, conducted at a frequency of 1 rad/s, are shown in Figure 2.3 [34].

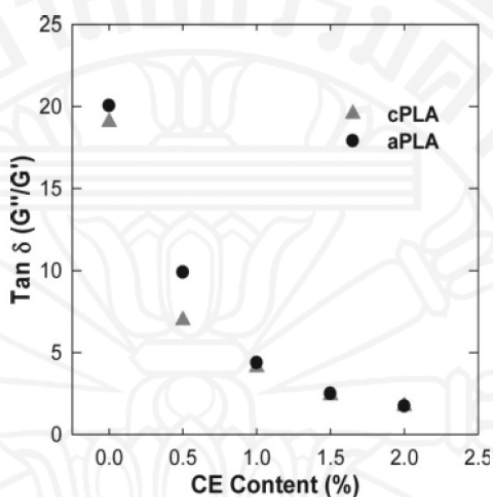


Figure 2.3 $\text{Tan } \delta$ values as a function of CE concentration at a frequency of 1rad/s for branched-extruded aPLA and cPLA samples [34].

Petchsuk et al., reported a lowering in complex viscosity (η^*), storage modulus (G'), loss modulus (G'') of *l*-PLLA after blending with multi-branched poly(D-lactide)s (mbPDLAs), prepared from ROP of D-lactide using polyglycidol (PG) as a macroinitiator. The blended products of a commercial grade *l*-PLLA with short arm length (mbPDLA101 and 201) copolymers derived from the feed ratios of LLA to PG at 10/1, 20/1. The results show suddenly drops in the complex viscosity (η^*), storage modulus (G'), loss modulus (G'') of the samples, compared to neat *l*-PLLA at all conducted temperatures. For the mbPDLA501, which was derived from the feed ratio of LLA to PG of 50/1. The copolymers with longer arm length show a difference flow patterns. The samples processed high complex viscosity (η^*), storage modulus (G'), loss modulus (G''). This is the effect from the formation of strong interaction, i.e., hydrogen bonding, between the 2 stereo constituents of lactate units. Rheology behaviors, in terms of complex viscosity (η^*), storage modulus (G'), loss modulus (G''), and $\text{tan}\delta$ of the blends, as a function of temperature of stereocomplex

blends containing different mbPDLAs, prepared at a 90/10ratio, are shown in Figure 2.4 [12].

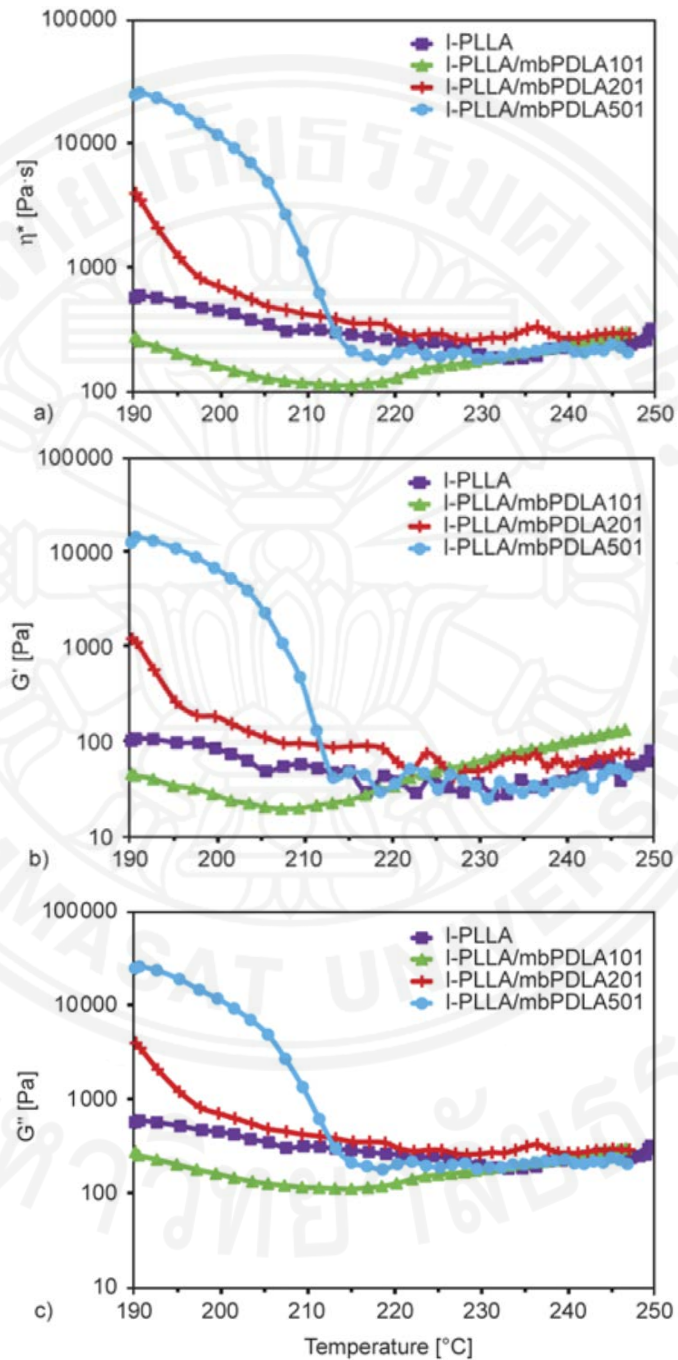


Figure 2.4 Temperature dependence of complex viscosity (η^*) (a), storage moduli (G') (b) and loss moduli (G'') and (c) of stereocomplex blends containing different mbPDLAs [12].

2.2.2.1 Synthesis of hyper-branched PLA

Hyper-branched PLA can be synthesized by ring-opening polymerization (ROP) of the cyclic dimer of lactic acid, lactide (LA), with a suitable catalyst and macroinitiator. Ouchi et al., successfully synthesized hyper-branched PLA by ROP using polyglycidol (PG), THF, and tin(II)ethylhexanoate as macroinitiator, solvent and catalyst, respectively. In the synthesis, reactor tubes and all reactants were dried in vacuum before use, in order to remove moisture and oxygen that may prohibit the polymerization. After drying PG and lactide, the freshly prepared tin(II)ethylhexanoate in THF was added to the tube. THF solvent was then allowed to evaporate in the vacuum system before purging with nitrogen again. The sealed reactor tube was placed in an oil bath with controlled temperature at 150 °C for 2 minutes, and subsequently to 115 °C with the reaction time of 24 hours. After the reaction was complete, dichloromethane was used as a solvent for dissolving the polymer products. It was then precipitated in a large amount of methanol to obtain hyper branched PLA. The structure and molecular weight of the synthesized products were investigated by NMR and GPC. The results show that molecular weight of hyper-branched PLLA can be controlled by varying the feed molar ratio of LLA to hydroxyl group of polyglycidol (M/OH). The blended films of the hyper-branched PLA, prepared by a solvent casting method showed a reduction of T_g when compared to *l*-PLLA. The T_g of hyper-branched PLA increased with an increase of molecular weight of hyper-branched PLA. In term of mechanical properties, the hyper-branched PLA films was more softer than linear PLLA (*l*-PLLA) sample (tensile strength 33.1 MPa, Young's modulus 1210 N/mm² and greater strain at break (14%)) with lower tensile strength (18.4 MPa), Young's modulus (504 N/mm²) and greater strain at break (163%) [2].

Petchsuk et al. successfully prepared multi-branched poly(D-lactide)s (mbPDLAs). The synthesis of mbPDLAs was performed by a ROP in bulk, using Sn(Oct)₂ catalyst and PG macro-initiator. Essentially, PG was dried in a reactor under vacuum. After drying, Sn(Oct)₂ (1 %wt of macro-initiator) was added, and the mixture was heated to 110°C for 1 hour. D-LA was added and reaction was further kept at 120°C for 24 hours. The feed ratios of LLA to PG were varied at 10/1, 20/1, and 50/1. Finally, the reaction mixture was dissolved in chloroform, and precipitated

in a large amount of ethanol to remove unreacted LLA and PG. Finally, powder precipitant of mbPDLAs were dried in a vacuum oven at 50°C for 24 hours [12].

It has been reported that not only hydroxyl groups, but also primary amine groups could initiate $\text{Sn}(\text{Oct})_2$ catalyzed ring opening polymerization of lactide [10, 11]. Zhang et al. synthesized hyper-branched PLLA by using polyethylene imine (PEI) as a macro initiator using $\text{Sn}(\text{Oct})_2$ catalyst at 130°C under N_2 atmosphere for 24 hours. In the presence of an initiator, primary or secondary hydroxyl or amino groups, linear polymers terminated with secondary hydroxyl groups are formed, whose molecular weight can be controlled through the variation in the feed ratios of monomer to initiator. The scheme for the synthesis of multi-arm star copolymers PEI-*b*-PDLA and PEI-*b*-PLLA is shown in Figure 2.5.

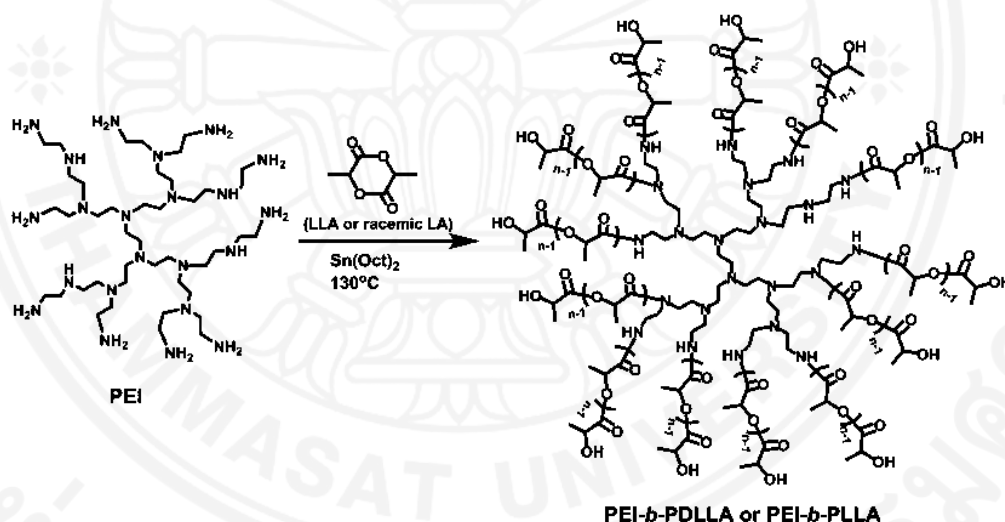


Figure 2.5 Scheme represents the synthesis of multi-arm star copolymers PEI-*b*-PDLA and PEI-*b*-PLLA

2.2.3 PLA blends

Polymers blends are combination of two or more different polymers with enhanced properties. The most importance characteristic of polymer blends is their phase behaviors. Polymer blends can exhibit either of miscible and immiscible phases. Most of the techniques used to characterize the miscibility of polymer blends are related to polymer transition behavior. The key property of the determination is the glass transition temperature (T_g). Miscible polymer blends exhibit a single T_g , generally between T_g of the two components. For the miscible systems, Fox equation

is a common equation used to predict the glass transition temperature of the polymer blend system.

$$\frac{1}{T_{gb}} = \frac{W_1}{T_{g1}} + \frac{W_2}{T_{g2}} \quad \text{Equation 1}$$

where, T_{gb} is glass transition temperature of the blend

W is weight fraction of the unblended component

T_g is glass transition temperature of the unblended component

Blending of PLA with other polymers is a useful strategy to improve the properties of PLA. Various polymers have been used for improving the properties of PLA, including elastomers, thermoplastic polymers, PEG, and copolymers of PLA. Amita Bhatia et al., studied thermal, mechanical and rheological properties of poly (lactic acid) (PLA) and poly (butylene succinate) (PBS) blends. The results show that blends containing up to 20wt% PBS contents in PLLA can improve their brittleness, flexural properties, heat distortion temperature and impact strength of the PLLA. This provided the advantages of the blends for use as food packaging, compost bags, and other biodegradable bags.

2.2.4 PLA Composites

Composites are defined as a macroscopic combination of two or more distance materials having an identifiable interface between them. There are two main components in composite systems which are matrix or binder and fillers. Matrix surrounds and binds fillers together, which is called reinforcement. Composite materials are widely used in many fields, such as, medical, automotive, and construction applications, because they are stronger, lighter and less expensive, compared to conventional materials. In general, engineering composited material is classified as composite building materials, reinforced plastics, metal composites and ceramic composites. In the last decade, composite preparation techniques have been applied to polymeric materials, which are known as polymer composites or reinforced plastics, with the advantages of non-corrosive, non-conductive, flexible, low

maintenance, long life, and design flexibility. Many types of fillers have been applied in the composite with PLA, in order to modify its mechanical, thermal, degradation and barrier properties such as whisker, nano clays and silica particles.

2.2.4.1 PLA/clays nanocomposites

Recently, many researchers have given considerable attention on polymer/clays nanocomposites for their unique properties, which may not be achieved by micro size fillers or other nano fillers [7, 35]. The individual layer thickness of layered silicates is in the order of 1 nm and their high aspect ratio (10 to 1000) causes the high interaction with polymer matrix. A few weight percent of layered silicates that are well distributed over the polymer matrix, therefore, provides much higher surface area for polymer-filler interaction than conventional composites [15].

In nanocomposites system, the nano clays are a part that carries the load or stress against straining from the external forces. Therefore, higher load resistance of solid clays can enhance the modulus of polymer matrix in well dispersion systems [36, 37]. High interfacial interactions contact leads to a better stress transfer in nanocomposites. Urbanczyk et al., had successfully prepared PLA/MMT-clays composites by in-situ polymerization in the presence of supercritical carbon dioxide (CO₂) [7]. The addition of clays leads to a decrease in the lactide polymerization rate, due to a significant sterically hindrance of clays at high loadings. However; the conversion can be improved by increasing the polymerization time and temperature. Cloisite®30B showed the highest reaction kinetics, as the hydroxyl groups and ammonium cations can act as polymerization initiators, so nano clays types affect the dispersion of clays in PLA/clays nanocomposites. In addition, a lowering in hydrophilicity on the surface of Cloisite®30B led to a better dispersion of clays, as reported by Prebe et al. [38]. In terms of mechanical properties, it has been reported that tensile modulus increased by increasing the fillers volume fraction in nanocomposites [30].

2.2.5 PLA/silica composites

Silica is an insoluble white powder; composed of Silicon (Si) and Oxygen (O) atoms in their structure with a chemical formula (SiO_2). There are two forms of silica which are quartz and colloidal, while the colloidal form is the most common one present in nature. In their structure, Si and O are linked by covalent bond, the Si with tetrahedral coordination bonded with 4 atoms of O leads to a high melting temperature of Silica, due to a strong covalence bond.

Silica composites are widely used in many fields today such as the use of carbon black and silica as reinforcing agents in elastomers. Silica sand is used in buildings and roads in the form of Portland cement, concrete, and mortar, as well as sandstone. Compatibility between PLLA and silica particles can be enhanced by modifying the silica surface. Various graft copolymers have been prepared for many enhancement including material compatibilization, improved mechanical property, metal adhesion, wettability control, dispersity, and thermal stability. Yan et al., successfully prepare PLA-*grafted*- SiO_2 . The PLLA chains are directly grafted onto a silicon surfaces by *in situ*-polymerization of Lactic acid [20]. The products are then compounded by using a Haake torque rheometer. DSC results show that PLLA-*grafted*- SiO_2 can accelerate a cold crystallization rate and increase a degree of crystallinity of PLLA. From shear rheology testing, it is indicated that PLA/PLA-*grafted*- SiO_2 nanocomposites are exhibits a typical homopolymer-like terminal behavior at low frequency range even at 5 wt % of PLA-*grafted*- SiO_2 content compared to PLA/ SiO_2 . It is also found that the nanocomposites show stronger shear-thinning behaviors in the high frequency regions after grafting. In addition, it shows an entanglement between grafted chains and matrix that is needed to improve the melt strength of PLLA from elongation viscosity testing.

Chapter 3

Methodology

3.1 Part 1 Synthesis and characterization of hyper-branched PLLA (*hb*PLLAs) and *l*-PLLA/ *hb*PLLAs blends.

3.1.1 Materials

L-Lactide and *l*-PLLA (4043D) were supplied by PURAC (Netherlands). Poly (ethylene imine) (PEI) ($M_n \sim 1,800$ by GPC and $M_w \sim 2,000$ by Light Scattering) was purchased from Aldrich (USA). Ethyl acetate, chloroform, ethanol, and toluene were purchased from Lab Scan (Thailand). Tin(II) octoate catalyst, $\text{Sn}(\text{Oct})_2$, was purchased from Wako (Japan). All chemicals were used without further purification.

3.1.2 Synthesis of *hb*PLLAs

*hb*PLLAs were synthesized by ROP using PEI as a macro-initiator and $\text{Sn}(\text{Oct})_2$ catalyst. The reaction was performed in a round-bottom flask, equipped with a condenser. The macro-initiator and monomer were first dried for 2 hours under vacuum before polymerization. The feed ratios of PEI to LLA were varied from 1:10, 1:20 and 1:100 by weight. Essentially, PEI was stirred at 70°C for 1 hour in the reaction flask, before dissolving in dried THF. $\text{Sn}(\text{Oct})_2$ catalyst was then added, and the mixture was stirred at 80°C for 2 hours, before adding LLA monomer. The polymerization was kept at 110 °C for 5 hours with continuous stirring. The mixture was finally dissolved in chloroform, and then precipitated in a large amount of methanol/hexane mixture to obtain solid *hb*PLLA products. The products were kept in a dry storage for further use. The products prepared from different feed ratios are referred to as codes, as summarized in Table 3.1.

Table 3.1 Summary on the synthesized *hb*PLLAs products.

Sample	PEI: LLA feed ratios (wt/wt.)
<i>hb</i> PLLA10	1:10
<i>hb</i> PLLA20	1:20
<i>hb</i> PLLA100	1:100

3.1.3 Preparation of *l*-PLLA/*hb*PLLAs blends

The synthesized *hb*PLLA products were blended with commercial *l*-PLLA by melt blending in an internal mixer (Chareon Tut, Thailand) at 170 °C for 20 minutes. The blend compositions of *hb*PLLAs were varies from 5, 10, 15, 20 % wt.

3.1.4 Characterizations of *hb*PLLAs and *l*-PLLA/ *hb*PLLAs blended films

3.1.4.1 Nuclear Magnetic Resonance (NMR) spectrometer

Chemical structures of *hb*PLLA products were investigated by an AVEN CEIII 500 MHz digital nuclear magnetic resonance (NMR) spectrometer (AV-500, Bruker Biospin), using CDCl₃ (for *hb*PLLAs) and D₂O (for PEI) solvents.

3.1.4.2 Differential Scanning Calorimeter (DSC)

Thermal property of the products was evaluated by Differential Scanning Calorimeter (DSC822e Mettler Toledo). The evaluation was performed by a heat-cool-heat standard method from -20 to 200°C, at a heating and cooling rate of 20°C/min. The first heating step is employed to erase the sample's thermal history.

The degree of crystallization is calculated by the following equation:

$$X_c = \frac{\Delta H_m}{\Delta H_m^\circ} \times 100\%$$

Where, ΔH_m is the enthalpy of melting and ΔH_m° denotes the enthalpy of fusion for the fully crystalline PLA, which has a value of 93.1 J/g.

The amount of overall crystallinity, (% crystallinity), which represents the crystallization formed during the cooling process at the employed conditions, was calculated using the following equation:

$$\% \text{ crystallinity} = \frac{\Delta H_m - \Delta H_c}{93.1} \times 100\%$$

Where, ΔH_m and ΔH_c are the enthalpy of melting and crystallization, respectively.

3.1.4.3 Universal Testing Machine (UTM)

Tensile behaviors of the blended films were examined on a Universal Testing Machine (Instron model 55R4502, Instron Corp., USA) with a 100 N load cell with a crosshead speed of 50 mm/min. The film samples were prepared by a hot-press compression molding machine (Chareon Tut, Thailand) at 170 °C for 15 minutes. The specimens were then prepared in a rectangular sheet form with 15 mm width and 100 mm gauge length, according to ASTM D882 procedures. At least five specimens were examined and averaged for each sample.

3.1.4.4 Rheometer

Dynamic rheological measurements were carried out using a strain-controlled rheometer (ARES, TA Inc., New Castle, USA) with a torque transducer capable of measurement over the range of 2–200 g.cm. The strain amplitude for dynamic measurements was fixed at 0.5%. The samples were prepared by a compression molding machine (Chareon Tut, Thailand) into a disc shape with a diameter of 25 mm and 1 mm thickness. The shear function mode for frequency dependence test was also performed from low to high shear forces, at a constant temperature of 180°C.

3.2 Part 2 Preparation and characterization of PCT-coated silica particles and *l*-PLLA/ PCT-coated silica composite films

3.2.1 Materials

Silica particles were extracted from RHA from a local mill in Ayutthaya province, Thailand. L-Lactid acid was purchased from Carlo Erba. PLA-*grafted*-Chitosan (PCT) copolymer was synthesized by condensation polymerization following the method in a previous report [32, 39]. Chitosan oligomers with 97% deacetylation were used in the reaction. *l*-PLLA resin (4043D, Natural Works Co. Ltd) was used as the polymer matrix in the preparation of *l*-PLLA/PCT-coated silica composite films.

3.2.2 Preparation of silica and PCT-coated silica particles

In the extraction of silica (SiO_2) particles, RHA raw material was first dried and ground to tiny particles by mechanical crushing. The particles were then dispersed in a NaOH solution. This method is called an alkaline extraction process. 1 M, of NaOH solution was used and mixed with RHA (50 g) with continuous stirring for 24 hours at 50°C. The product obtained from this step is sodium silicate (Na_2SiO_3) solution. The sol-gel method was subsequently applied in order to convert the solution into silica particles. In this step, CO_2 gas was flowed through the solution at a flow rate of 2.0 L/min. The pH of the solution was adjusted to 7 by washing with a large amount of water. The remaining gels were dried and mechanically crushed to obtain silica particles product.

In a separate process, the size reduction without the use of mechanical crushing step and surface modification of silica (SiO_2) particles were performed in a single step process by adding of a PCT polymeric surfactant (10% wt of RHA) into the Na_2SiO_3 solution. The mixture was then ultra-sonicated for 30 min, in which CO_2 gas was flowed through the solution at a flow rate of 2.0 L/min. Finally, PCT-coated silica (SiO_2) particles were precipitated in dichloromethane. The fine dried powder products were obtained by drying in an oven followed by gentle grinding.

3.2.3 Preparation of *l*-PLLA/ PCT-coated silica composites

The *l*-PLLA/ PCT-coated silica composites films were prepared by melt blending in an internal mixer (Chareon Tut, Thailand). Two types of particles were dispersed in *l*-PLLA resin (4043D) to produce their respective composites. The mixing temperature was set at 170 °C with a rotor speed of 50 rpm for 15 minutes. The composition of PCT-coated silica particles were varied from 0-2.0 wt%. The polymer films were prepared by hot-press compression molding machine (Chareon Tut, Thailand) at 170 °C for 15 minutes. The specimens were prepared in rectangular sheet form with a 15 mm width and 100 mm of gauge length, according to ASTM D882.

3.2.4 Characterization of PCT-coated silica and *l*-PLLA/PCT-coated silica composite films

3.2.4.1 Fourier Transform Infrared (FTIR) spectroscopy

FTIR analysis was used to study the chemical interaction between PCT and silica within the coated particles. FTIR spectra were recorded on a Nicolet 6700 FTIR spectrometer in a transmission mode with a resolution 2 cm⁻¹ by co-adding 32 scans. The samples were prepared as pellet by mixing with KBr matrix at 2% wt. composition.

3.2.4.2 Scanning Electron Microscopy (SEM)

To observe surface morphology of the coated silica particles, an SEM (S3400N, Hitachi Co.) was applied. The samples were prepared with a platinum coating technique.

3.2.4.3 Nitrogen gas sorption technique

Nitrogen gas sorption technique was used to estimate the particle size and surface area of PCT-coated silica particles. The measurements were performed by an Autosorb-1(Quantachrome).

3.2.4.4 Quantachrome

An ultra-pycnometer 1000 (Quantachrome) was used in the measurement of their average density.

3.2.4.5 Universal Testing Machine (UTM)

Tensile behavior of the neat *l*-PLLA, *l*-PLLA/PCT-coated silica at various PCT-coated silica compositions were studied by using a Universal Testing Machine (Instron model 55R4502, Instron Corp., USA) with a 100 N load cell with a crosshead speed of 50 mm/min at 170°C. At least five specimens were examined for each test.

3.2.4.6 Gas permeability analysis

The samples were prepared as film by compression molding (thickness ~100 μm) according to the conditions reported earlier [40]. Water vapor permeability of the neat *l*-PLLA and *l*-PLLA/PCT-coated silica composite films at various PCT coated silica compositions were studied at 38 °C, 90% relative humidity and 1 atm pressure. The measurements were conducted on an Illinois Instrument (Model 7200), according to ASTM F1249-01. Oxygen permeability was measured at 23°C and 0% relative humidity. On a Mocon Instrument (Ox-Tran Model 2/21), following ASTM D3985. Carbon dioxide permeability was also examined at 23°C and 0% relative humidity on a Mocon Instrument (Permatran-C Model 4/41).

Chapter 4

Results and Discussion

4.1 Part 1 Synthesis and characterization of hyper-branched PLLA (*hb*PLLAs) and *l*-PLLA/ *hb*PLLAs blended.

4.1.1 Chemical structure of *hb*PLLAs (NMR)

Chemical structure of *hb*PLLA products are examined by NMR spectroscopy. ¹H NMR spectrum of *hb*PLLA10 derived from a 1:10 weight ratio of PEI: LLA is compared with that of PEI macro-initiator in Figure 4.1. The spectrum shows characteristic chemical shifts at 5.13 ppm (a, b), assigned to methine protons in the main-chain repeat units, with the integration value of 1.00. The signal at 4.32 ppm (c) is assigned to methine protons in terminal units of *hb*PLLA, whose integration is 0.098. The chemical shifts at 1.55 ppm (d, e) are assigned to the methyl groups of PLLA. A broad signal covering the region of 2-3 ppm is associated with CH₂ protons of PEI. NMR results also allow for the determination of chemical structures of the products, in terms of LLA arm lengths and PLLA/PEI molar ratios by using the integration values these characteristic signals. The data used in the calculation of average branch length are the integration values of signals at 5.1 and 4.3. The results are summarized in Table 4.1.

Table 4. 1 Results on average LLA lengths and PLLA/PEI molar ratio in *hb*PLLAs chains

Sample	PEI: LLA feed ratios	Average LLA branch length (units)	PEI :LLA molar ratios (in chain)
<i>hb</i> PLLA10	1:10	10	1:5
<i>hb</i> PLLA20	1:20	12	1:9
<i>hb</i> PLLA100	1:100	19	1:11

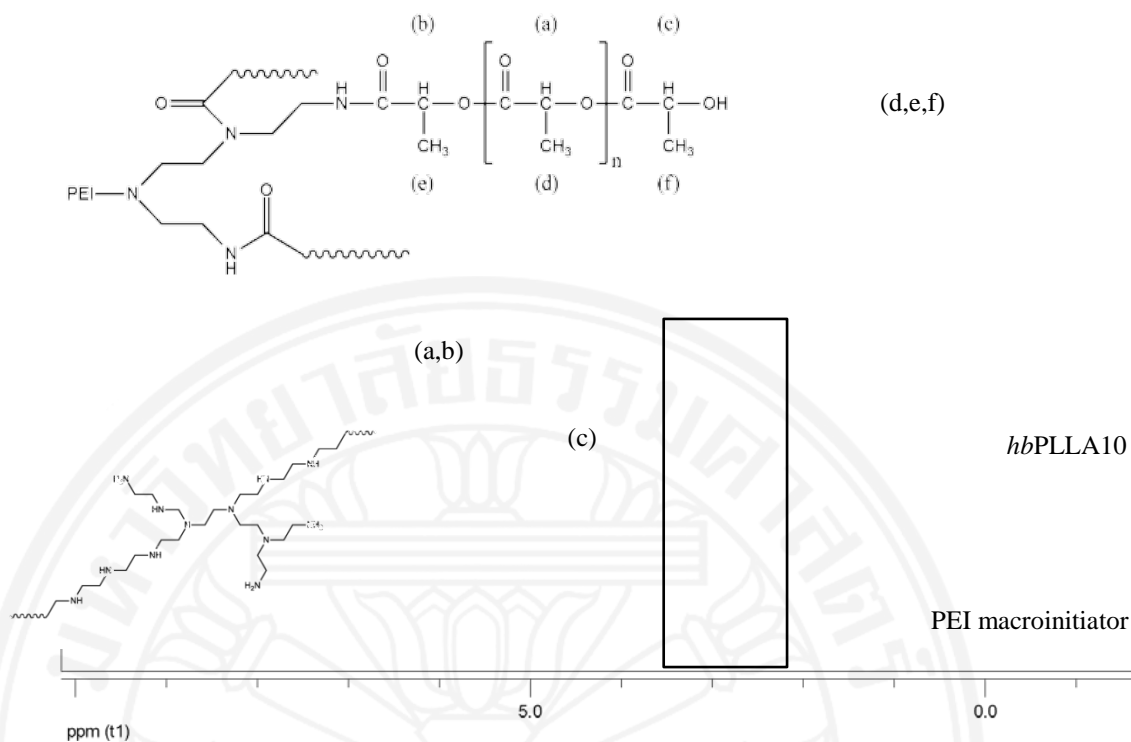


Figure 4.1 ¹H-NMR spectra and chemical structures of *hbPLLA10* and PEI

The data used in the calculation of PLLA/PEI are the signals around 2-3 ppm (PEI protons) and the signals at 5.1 (protons of PLLA unit) for 1:10, 1:20 and 1:100 for PEI:LLA feed ratio. The calculation of PLA/PEI ratios of the product derived from 1:10, 1:20, and 1:100 PEI:LLA feed ratio are shown below.

hbPLLA10

$$\begin{aligned} \text{Proton signals of PEI} &= \frac{12-3}{4 \text{ protons}} \\ &= \frac{0.509+0.301}{4} \\ &= 0.203 \end{aligned}$$

Therefore, 1 proton of PEI calculated as 0.203

$$\begin{aligned} \text{Proton signals of PLLA} &= \frac{15.134}{1 \text{ proton}} \\ &= \frac{1.000}{1} \\ &= 1.000 \end{aligned}$$

Therefore, one proton of PLLA calculated as 1.000

Calculation of PLLA/PEI molar ratio

$$\frac{\text{Proton signal of PLLA}}{\text{Proton signal of PEI}} = \frac{1.000}{0.203}$$
$$= 5$$

hbPLLA20

$$\text{Proton signals of PEI} = \frac{12-3}{4 \text{ protons}}$$
$$= \frac{0.439}{4}$$
$$= 0.1097$$

Therefore, 1 proton of PEI calculated as 0.203

$$\text{Proton signals of PLLA} = \frac{15.134}{1 \text{ proton}}$$
$$= \frac{1.000}{1}$$
$$= 1.000$$

Therefore, one proton of PLLA calculated as 1.000

Calculation of LLA/PEI molar ratio

$$\frac{\text{Proton signal of PLLA}}{\text{Proton signal of PEI}} = \frac{1.000}{0.1097}$$
$$= 9$$

hbPLLA100

$$\text{Proton signals of PEI} = \frac{12-3}{4 \text{ protons}}$$
$$= \frac{0.357}{4}$$
$$= 0.0892$$

Therefore, 1 proton of PEI calculated as 0.203

$$\text{Proton signals of LLA} = \frac{15.134}{1 \text{ proton}}$$
$$= \frac{1.000}{1}$$
$$= 1.000$$

Therefore, one proton of LLA calculated as 1.000

Calculation of LLA/PEI molar ratio

$$\frac{\text{Proton signal of LLA}}{\text{Proton signal of PEI}} = \frac{1.000}{0.0892}$$
$$= 11$$

4.1.2 Thermal property (DSC)

Thermal properties of the resulting *hbPLLAs* are examined, in which their DSC thermograms are shown in Figure 4.2. The results indicate that the properties are strongly dependent on the polymer's chemical structures. *hbPLLA* with short LLA arm's length (i.e. *hbPLLA10* and *hbPLLA20*) are completely amorphous, as no crystalline characteristics are observed in their DSC thermograms. In contrast, the copolymer with longer arm's lengths (i.e. *hbPLLA100*) processes a semi-crystalline structure, where the melting characteristic peak (T_m) is observed at 162°C. The glass transition temperature (T_g) of the hyper-branched copolymer increases with the length of LLA sequences from 36 to 47°C, as a result from a decrease in the chain flexibility.

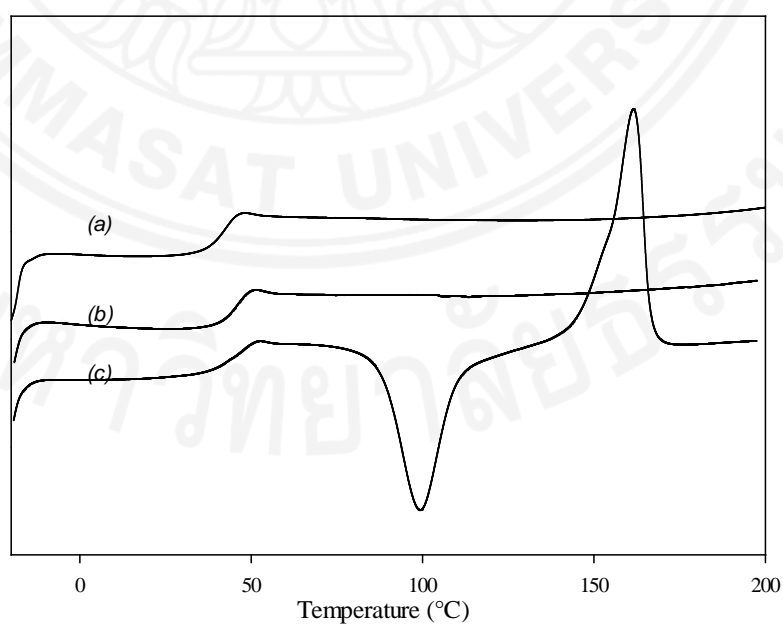


Figure 4.2 DSC thermogram (2nd heating scan) of (a) *hbPLLA10*, (b) *hbPLLA20* and (c) *hbPLLA100* samples.

Thermal properties of *l*-PLLA/*hb*PLLA blends containing various types of *hb*PLLAs and as a function of the blend compositions are investigated. All blends show lower T_g and T_m than neat *l*-PLLA. Both T_g and T_m values decrease with an increase in the *hb*PLLA content, and also increase when the LLA arm's length further increases.

DSC thermograms of *l*-PLLA/*hb*LLA10 and *l*-PLLA/*hb*LLA20 blends as a function of the blend compositions are shown in Figure 4.3 and 4.4, respectively. Single T_g is observed in all samples, indicating complete miscible blend systems at all compositions. No melting characteristic peak is observed in the thermogram of *hb*PLLA10 and *hb*PLLA20, due to its short LLA arm length, while neat *l*-PLLA exhibits a typical T_m at 150°C. Upon adding of *hb*PLLAs, a decrease in ΔH_m value of the blends is observed. The degree of reduction in the values increase with an increase in the *hb*PLLA10 contents, from 5 to 20 %wt, reflecting that this short-branched structured material has high synergic effect with the *l*-PLLA matrix, which inhibits the crystal formation of the *l*-PLLA domains, and hence lower crystalline contents.

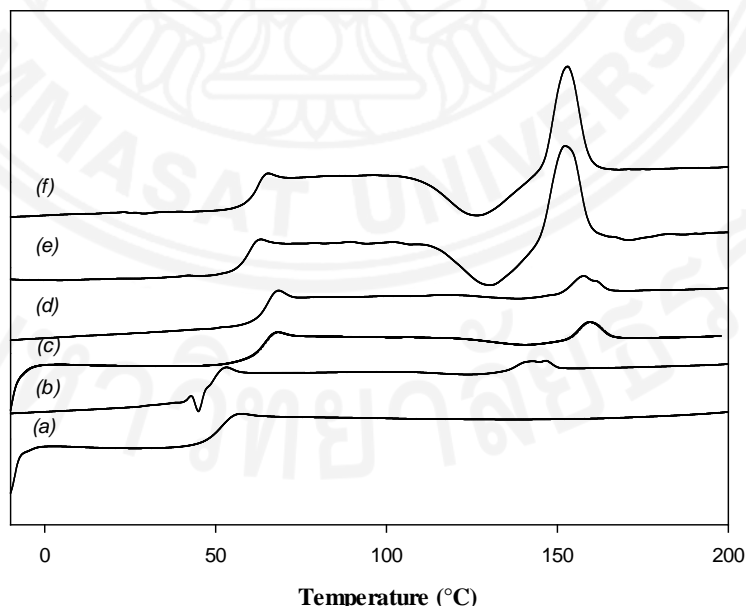


Figure 4.3 DSC thermograms (2nd heating scan) of (a) *hb*PLLA10 and *l*-PLLA/*hb*PLLA10 blends at various compositions %wt: (b) 80/20, (c) 85/15, (d) 90/10, (e) 95/5, and (f) *l*-PLLA.

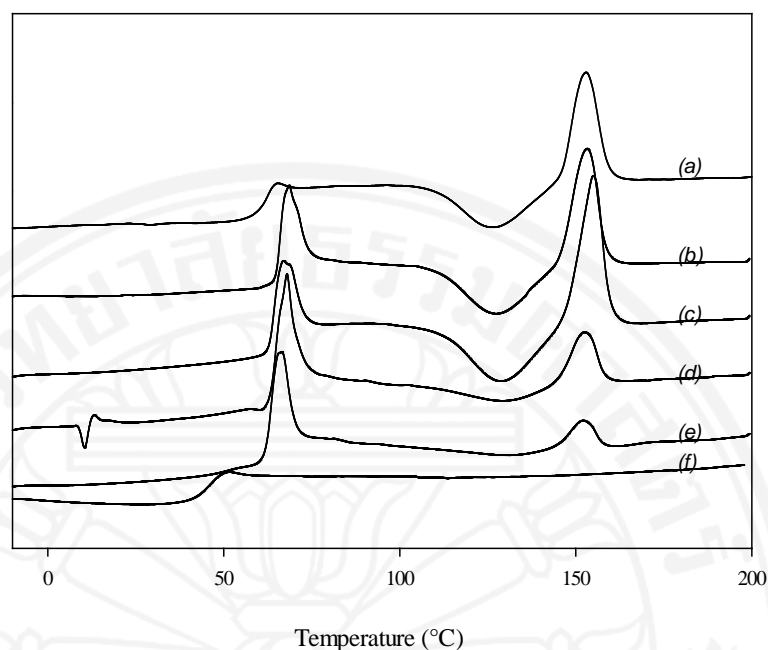


Figure 4.4 DSC thermograms (2nd heating scan) of (a) *hb*PLLA20 and *l*-PLLA/*hb*PLLA20 blends at various compositions %wt: (b) 80/20, (c) 85/15, (d) 90/10, (e) 95/5, and (f) *l*-PLLA.

The corresponding DSC thermograms of blends consisting of *hb*PLLA100, which possess long LLA sequences, are shown in Figure 4.5. Single T_g is also observed in all blend samples, reflecting complete miscible blend systems. The *hb*PLLA100 exhibits a T_m at 162 °C, which is higher than that of neat *l*-PLLA. This is likely because its crystalline domains are derived from close packing of branches with optimum length as the results from the stiff PEI core. When the copolymer is blended with *l*-PLLA, double T_m peaks appear at the temperatures, correspond those of the 2 components. This indicates a formation of 2 distinct crystalline domains originated from *hb*PLLA100 and the *l*-PLLA matrix.

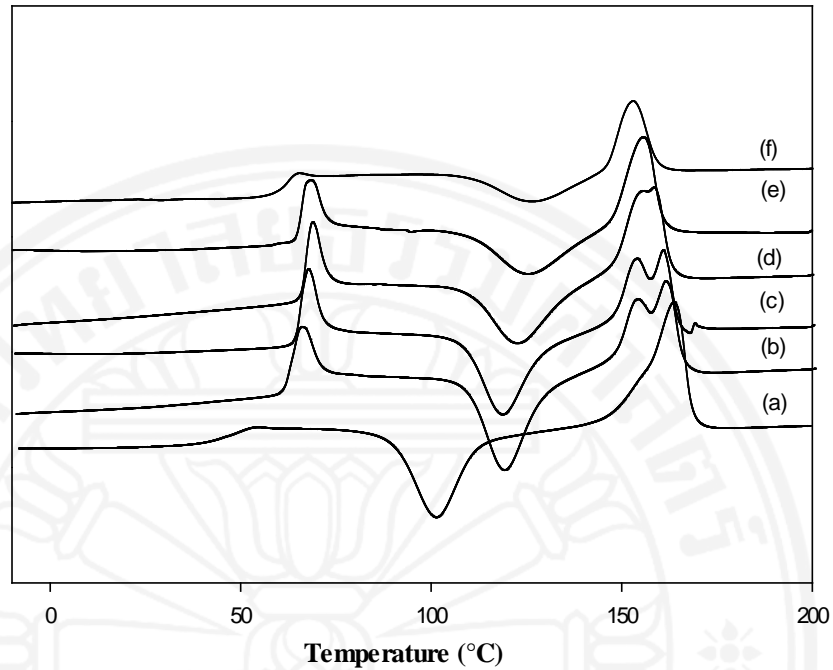


Figure 4.5 DSC thermograms (2nd heating scan) of (a) *hb*PLLA100 and *l*-PLLA/*hb*PLLA100 blends at various compositions %wt: (b) 80/20, (c) 85/15, (d) 90/10, (e) 95/5 and (f) *l*-PLLA.

One of the key characteristics of polymer blends is their miscibility, which can be observed from transition behaviors, especially the glass transition temperature (T_g). Single phase or miscible polymer blends exhibit a single T_g , generally is between T_g 's of the 2 components. For miscible systems, Fox equation is applied to predict the glass transition temperature of the polymer blends, as shown in equation 1.

$$\frac{1}{T_{gb}} = \frac{W_1}{T_{g1}} + \frac{W_2}{T_{g2}} \quad \text{equation 1}$$

where, T_{gb} is glass transition temperature of the blend

W is weight fraction of the blend component

T_g is glass transition temperature of the blend component

The calculation of expected T_g by using the Fox equation and their thermal properties of *l*-PLLA/*hb*PLLA10, *l*-PLLA/*hb*PLLA20, and *l*-PLLA/*hb*PLLA100 blended films are summarized in Table 4.2, 4.3 and 4.4, respectively. The calculated are compared with those (T_g) of the blend samples. The observed values are lower than those of the blend systems containing shorter *hb*PLLA, reflecting weaker specific interaction between the blend consistent. However, the corresponding values for the *hb*PLLA100 system are almost identical to the values from theory. This indicates strong specific interaction between the two components, due to their high degree of miscibility.

Table 4.2 Thermal properties of *l*-PLLA/*hb*PLLA10 blends

Blend ratios	T_{gb} [°C]	T_g [°C]	T_c [°C]	T_m [°C]	ΔH_c [J/g]	ΔH_m [J/g]
<i>l</i>-PLLA	62	62	127	153	16.8	14.7
95/5	59	60	131	152	14.8	14.5
90/10	58	55	129	151	1.4	2.4
85/15	56	54	132	148	2.1	1.9
80/20	54	48	125	147	1.2	1.4
<i>hb</i>PLLA10	37	37	-	-	-	-

Table 4.3 Thermal properties of *l*-PLLA/*hb*PLLA20 blends

Blend ratios	T_{gb} [°C]	T_g [°C]	T_c [°C]	T_m [°C]	ΔH_c [J/g]	ΔH_m [J/g]
<i>l</i>-PLLA	62	62	127	153	16.8	14.7
95/5	61	60	129	154	14.1	15.6
90/10	60	59	130	153	13.0	13.1
85/15	59	58	131	152	1.8	2.1
80/20	58	57	-	151	-	1.0
<i>hb</i>PLLA20	46	46	-	-	-	-

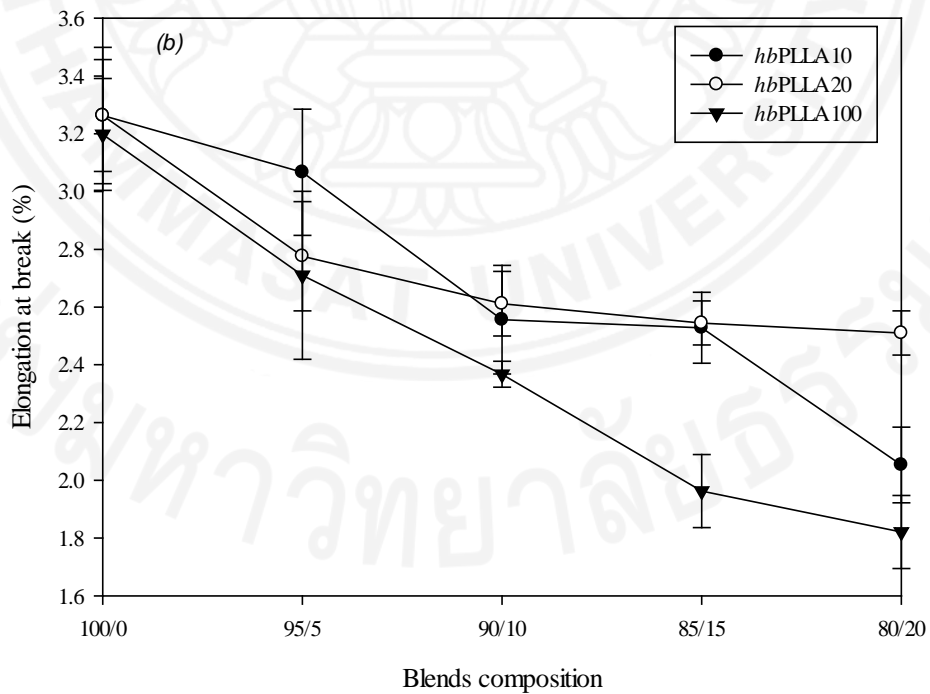
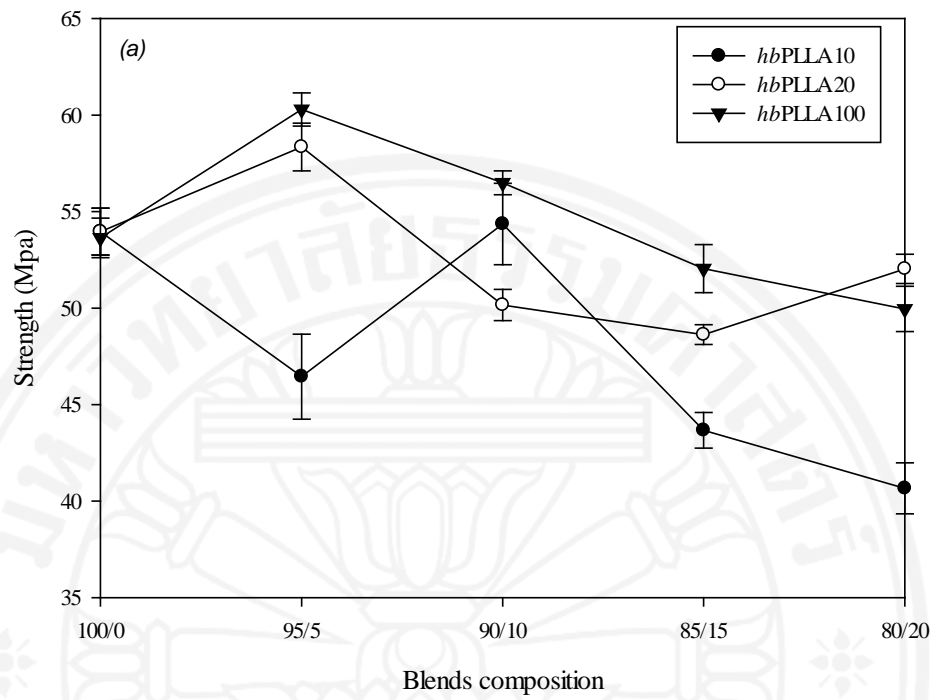
Table 4.4 Thermal properties of *l*-PLLA/*hb*PLLA100 blends

Blend ratios	T _{gb} [°C]	T _g [°C]	T _c [°C]	T _m [°C]	Δ H _c [J/g]	Δ H _m [J/g]
<i>l</i>-PLLA	62	62	127	153	16.8	14.7
95/5	61	61	126	154	20.8	21.4
90/10	60	60	122	153	26.2	27.2
85/15	59	59	119	154	29.8	29.9
80/20	58	58	121	154	31.4	32.7
<i>hb</i>PLLA100	47	47	100	162	34.7	40.0

*T_{gb} is T_g value of the blends calculated by the Fox equation.

4.1.3 Mechanical property (UTM)

The tensile properties of *l*-PLLA/*hb*PLLA blend films are summarized in Figure 4.6. Figure 4.6a show that, the *hb*PLLAs with long arm's length (*l*-PLLA/*hb*PLLA100 blend film) show highest tensile strength, which is likely due to the effect from chain entanglements. This is observed in all *hb*PLLA100 composition compared to those of the shorter arm's lengths. Due to the highly branched of globular structure, the configuration of copolymer with short arm's length is coined resulting in a poor mechanical strengths.



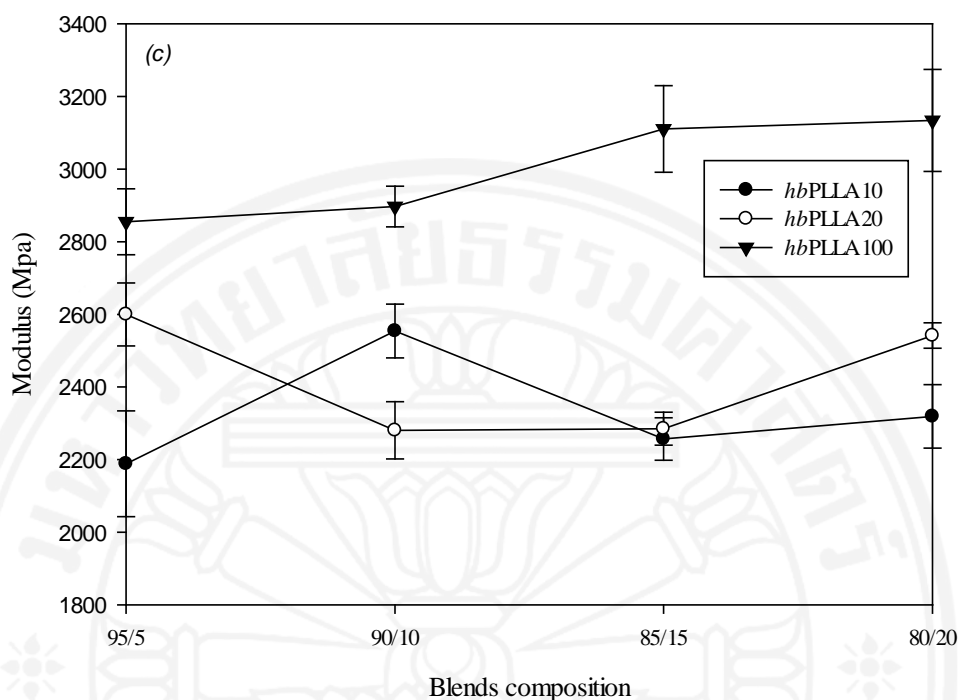


Figure 4.6 Tensile strength (a), Elongation at break (b) and Modulus (c) of *hb*PLLAs and *l*-PLLA/*hb*PLLAs blends films, as a function of the blend composition

In contrast, an opposite trend is observed in elongation at break values of the samples, as shown in figure 4.6b. The *l*-PLLA/*hb*PLLA100 blended films show the lowest elongation at break at all *hb*PLLA100 compositions due to the chain stiffness imposed by the PEI core of the hyper-branched components. The mechanism of semi-crystalline polymers during the applied tension force is the alignment of amorphous domains. When the chains are straighten, the additional stress causes necking in which the chains continues to slide and deform. The blends contain the hyper-branched structure with long arm's length (ie; *l*-PLLA/*hb*PLLA100 blends film) show an increase in the modulus values with the increase in the *hb*PLLA100 compositions. For the short arm's lengths (ie; *l*-PLLA/*hb*PLLA10 and *l*-PLLA/*hb*PLLA20 blends film) show slightly change at all *hb*PLLAs composition. Those results are the effect from the high density and crystallinity of the blends due to the long arm's length of *hb*PLLA100.

4.1.4 Rheology

The complex viscosity, of *l*-PLLA/*hb*PLLAs blends (at a composition of 90/10) as a function of shear rate are shown in Figure 4.7a. The results indicate that all blends have lower complex viscosity than that of neat *l*-PLLA, as of result from the addition of the branch-structured component. The lowest values are observed in the blend containing *hb*PLLA20. From NMR results, it is very clearly observed that *hb*PLLA10 possesses shortest LLA sequences. However the blend of this copolymer shows higher complex viscosity than the *l*-PLLA/*hb*PLLA20 blend. This is likely due to the effect of the strong hydrogen bonding interaction between nitrogen atoms of PEI core and *l*-PLLA. As the branch length of *hb*PLL10 is much shorter, the exposure of the PEI core to *l*-PLLA is more than the *hb*PLLA20 counterpart, because of lower degree of steric hindrance from the LLA branches. In the blends containing *hb*PLLA100 with longer arm's length, the complex viscosity is much higher, because the LLA branches lengths are long enough to allow entanglements between the hyper-branched and *l*-PLLA chains, and the effect of arm's length is more dominant than the interaction formed by nitrogen atom of PEI core.

Effects of blend compositions on rheological property of the blend are also examined by using the *l*-PLLA/*hb*PLLA20 blend system. The complex viscosity decrease with an increase in the *hb*PLLAs compositions. The complex viscosity of this blend system (at a various blends composition), as a function of shear rate are shown in Figure 4.7b. The complex viscosity decreased with an increase in the *hb*PLLAs compositions. This is because *hb*PLLAs can act as a plasticizer for disentanglement of the polymer chains, resulting in the lower complex viscosity. Insight into the origin of this property is essential, and can be applied in many applications, especially in optimizations of flow behaviors of *l*-PLLA during its processing and fabrication processes. Therefore, *hb*PLLAs with different structures can be employed as processing aids.

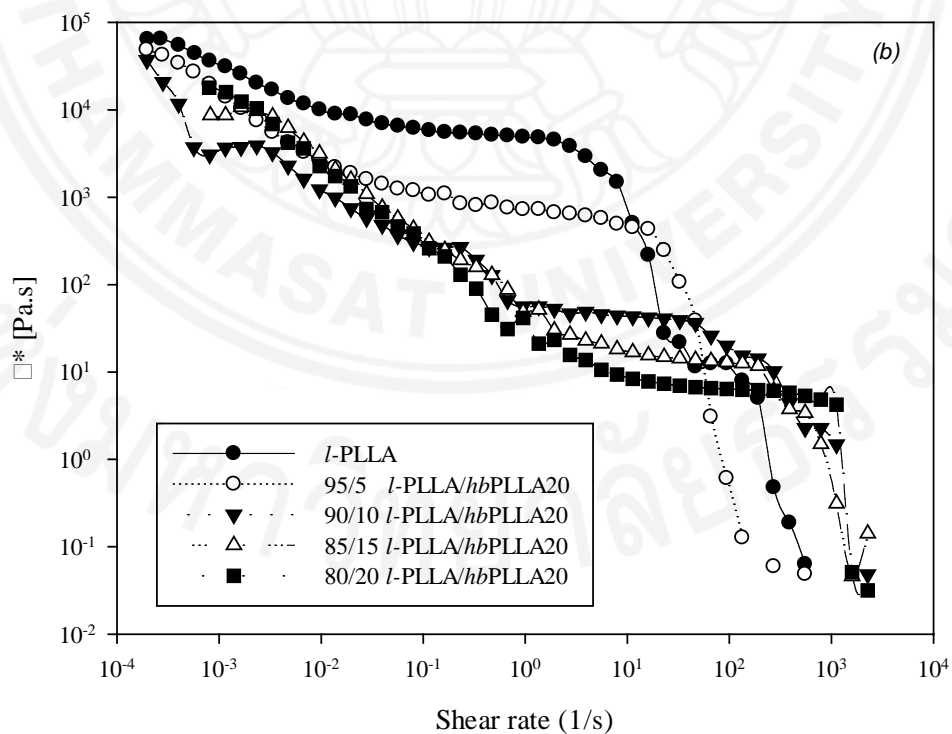
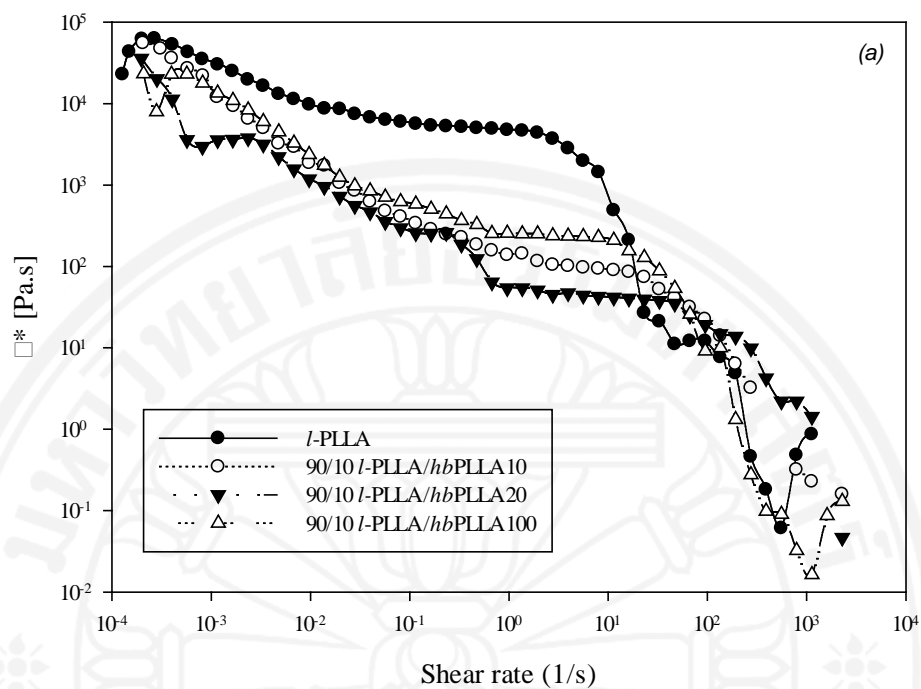
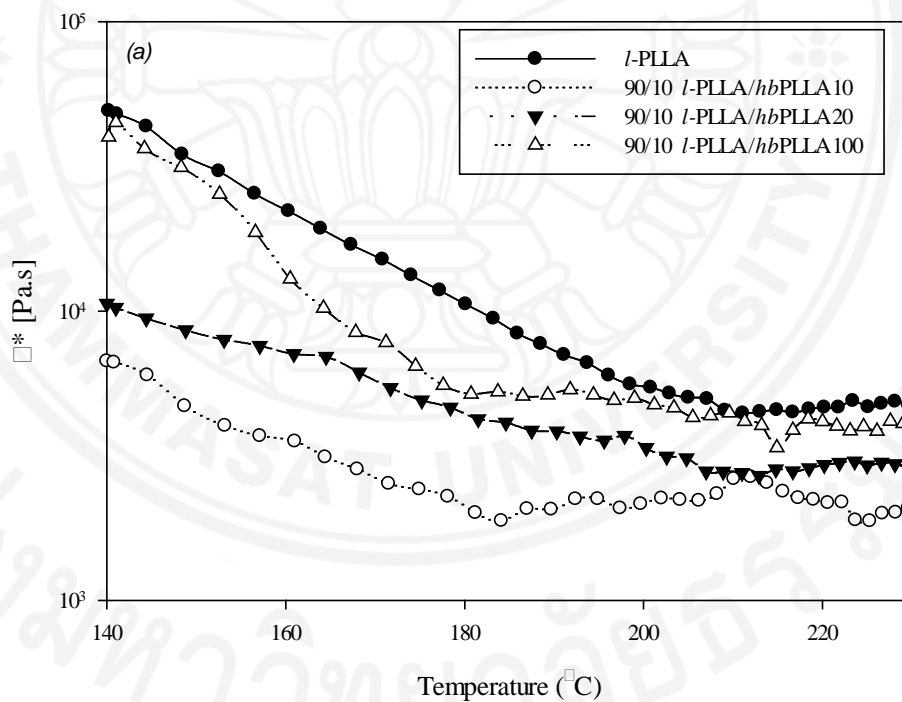


Figure 4.7 Complex viscosity, as a function of shear rate of (a) *l*-PLLA/*hb*PLLAs blends containing different *hb*PLLAs, at a 90/10 composition and (b) *l*-PLLA/*hb*PLLA20 blends (at a various blend compositions)

In the study of temperature dependence behavior, dynamic rheological measurements are conducted at strain amplitude 0.5% in the temperature range of 140-240 °C in order to study effects of branched structure on the viscoelastic properties. Complex viscosity (η^*), storage modulus (G'), and loss modulus (G'') of *l*-PLLA/*hb*PLLAs blends containing different *hb*PLLAs, at a 90/10 composition are shown in Figure 4.8. At temperatures below T_m of the blend components, the blends consisting hyperbranched of shorter arm's length, ie; *hb*PLLA10 and *hb*PLLA20 show lower complex viscosity, storage modulus, and loss modulus, compared to *l*-PLLA, as the materials act as a plasticizer for *l*-PLLA matrix. The blends of the long arm's length ie; *l*-PLLA/*hb*PLLA100 blend sample shows similar trends of properties with neat *l*-PLLA.



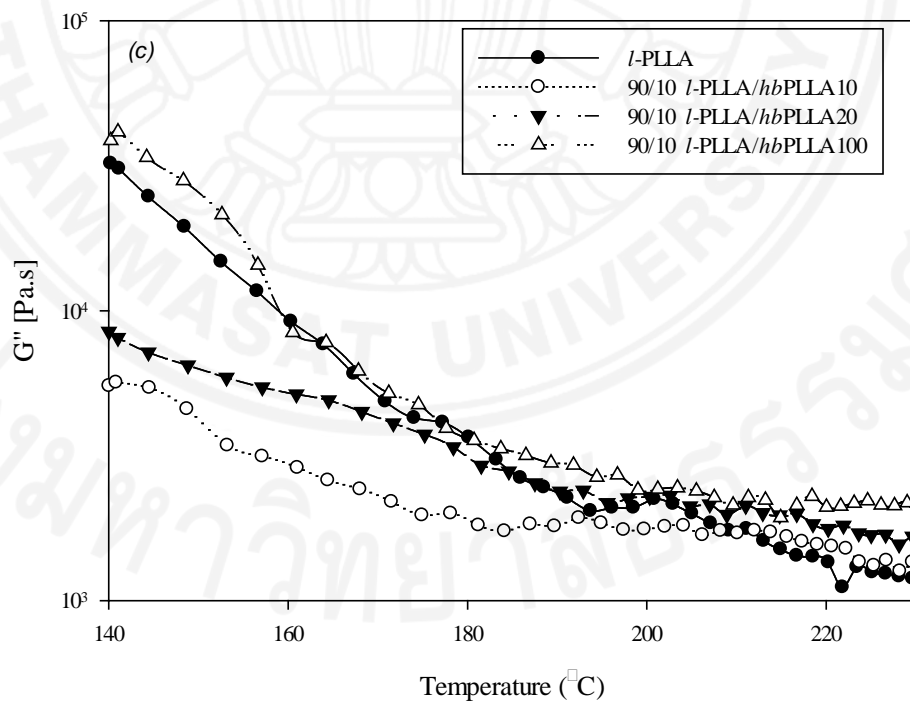
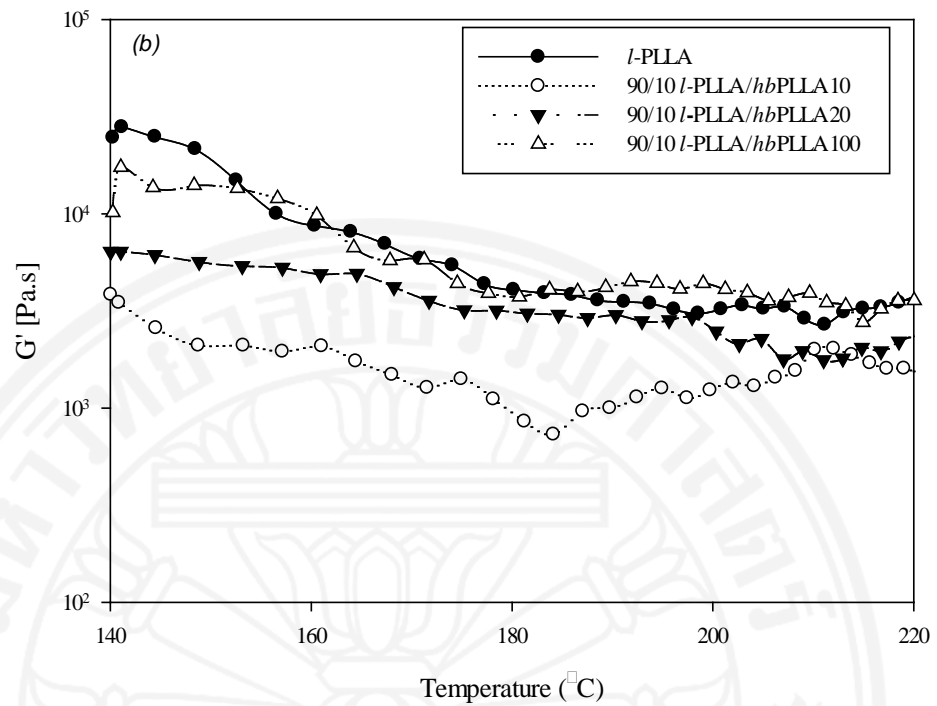
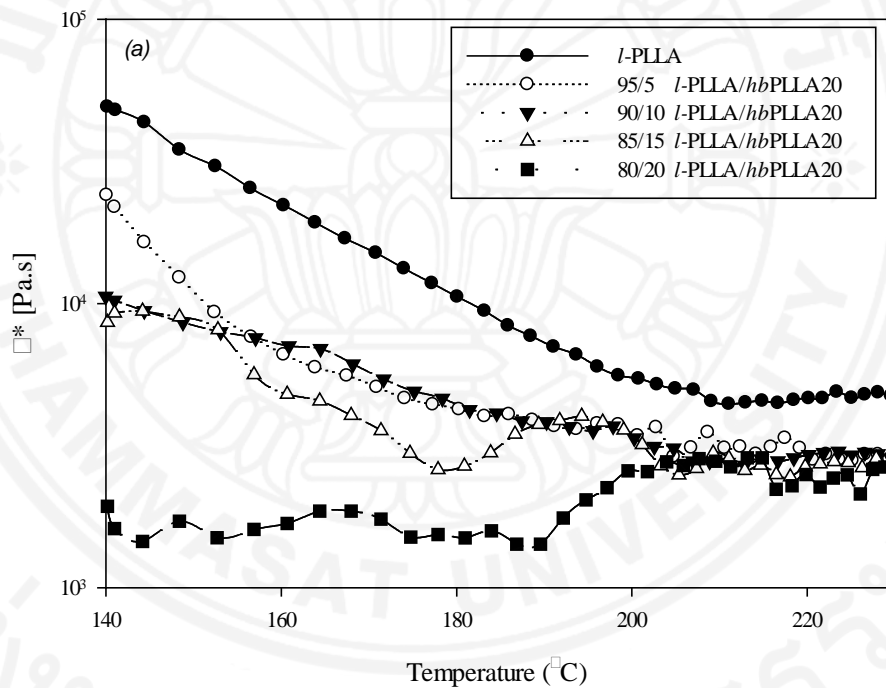


Figure 4.8 Viscoelastic characteristics in terms of (a) complex viscosity (η^*), (b) storage modulus (G') and (c) loss modulus (G'') as a function of temperature of *l*-PLLA/*hb*PLLAs blends at a 90/10 composition.

The viscoelastic behaviors are measured as function of temperature by using strain amplitude of 0.5% in the temperature range of 140-230 °C. Viscoelastic characteristics in terms of (a) complex viscosity (η^*), (b) storage modulus (G') and (c) loss modulus (G'') as a function of temperature of *l*-PLLA/*hb*PLLA20 blends (at a various blends composition) are shown in Figure 4.9. All blends show lower complex viscosity (η^*), storage modulus (G') and loss modulus (G'') than the *l*-PLLA at all temperatures. This is likely because the *hb*PLLAs can act as plasticizer for *l*-PLLA by retarding its chain entanglement. This characteristic enables the use of as processing enhancement additive in the fabrication of *l*-PLLA.



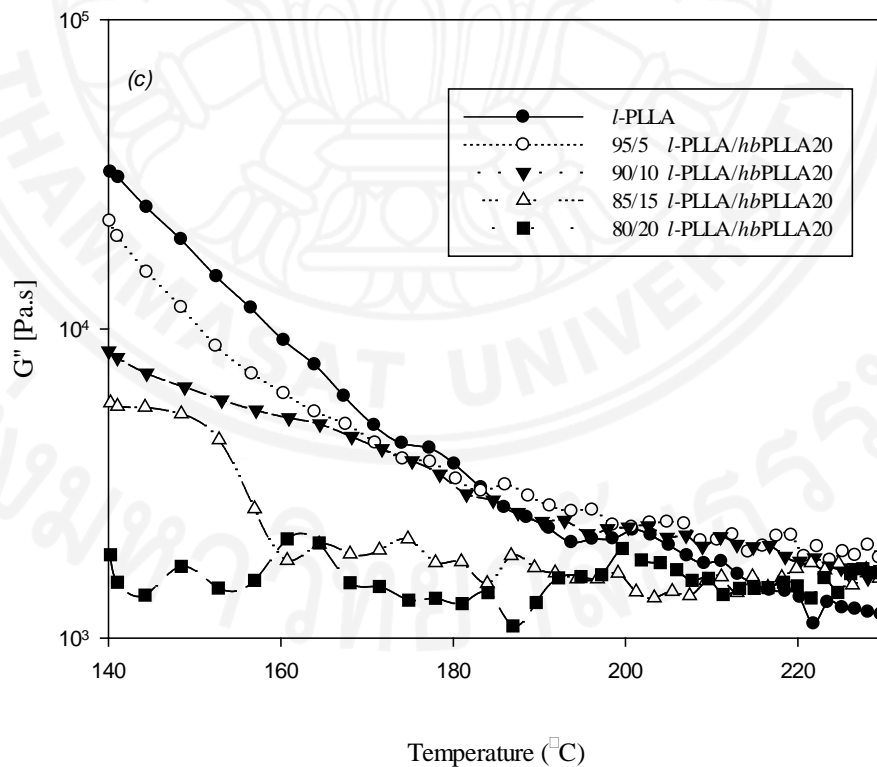
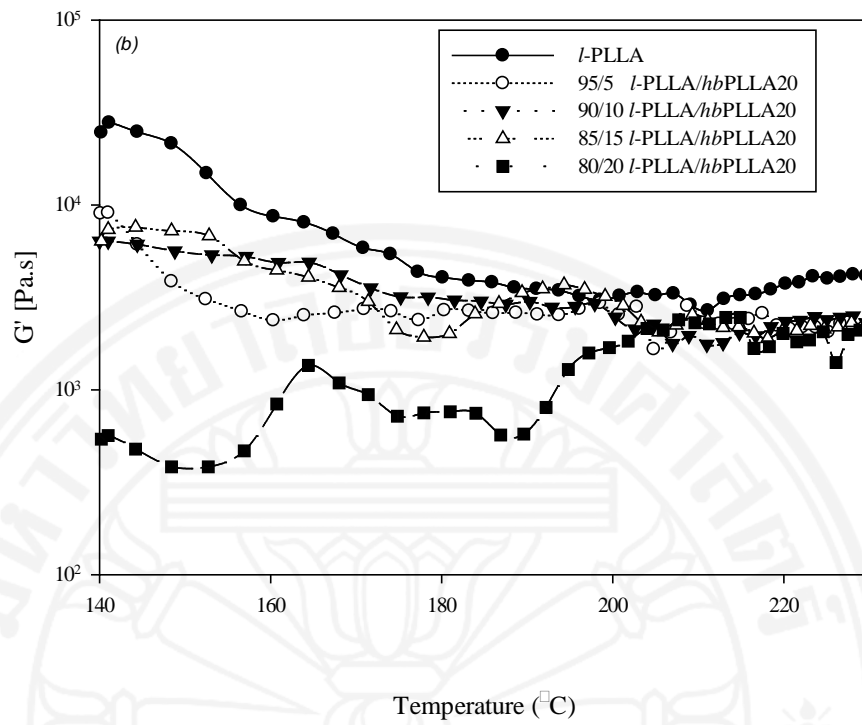


Figure 4.9 Viscoelastic characteristics in terms of (a) complex viscosity (η^*), (b) storage modulus (G') and (c) loss modulus (G'') as a function of temperature of *l*-PLLA/*hb*PLLA20 blends (at a various blends composition).

4.2 Part 2 Preparation and characterization of PCT-coated silica particles and *l*-PLLA/ PCT-coated silica composite films

Silica particles are prepared from raw materials from agriculture waste, i.e. RHA. The preparation of the silica particles as a single step process is developed. The materials are characterized and used in the preparation of *l*-PLLA/PCT-coated silica composites films.

4.2.1 Chemical structure (FTIR)

Chemical structures of silica and PCT-coated silica particles were studied by FTIR. FTIR spectra of silica and PCT-coated silica particles are shown in Figure 4.10. Band centered at 1635 cm^{-1} was a characteristic of uncoated silica particles, belong to hydroxyl groups (-OH bending). The peak at 1100 cm^{-1} is due to Si-OH stretching mode. The vibrational mode of silica units with O terminals appears at 850 cm^{-1} , with a sharp band, but weak intensity. In addition, there are some organic compounds remaining on silica particles, reflecting by the characteristic band at 1470 cm^{-1} ($\text{-CH}_2\text{-}$ bending). The corresponding spectrum of PCT-coated silica particles (Figure 4.9a) show characteristic band at 1775 cm^{-1} , assigned to the carbonyl group of PLA (C=O stretching mode). The difference spectrum (Figure 4.10c) obtained from PCT-coated silica and neat silica particles shows a broad peak around 1590 cm^{-1} and strong sharp band at 1105 cm^{-1} . Negative difference patterns located at 1010 and 850 cm^{-1} reflect the interaction between silicate terminals with the coating PCT polymer. Strong interaction like hydrogen bonding is formed, leading to a reduction in the bands intensity of the silica characteristic mode.

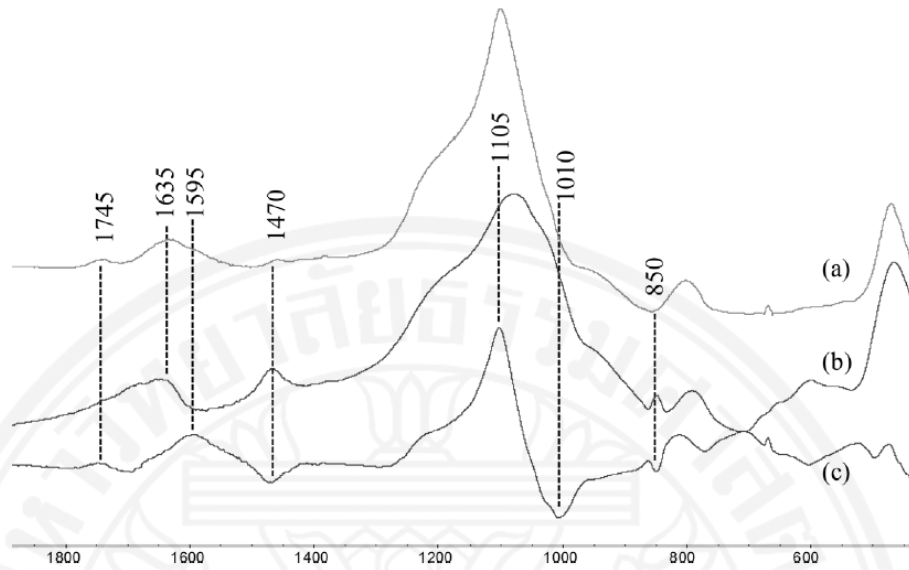


Figure 4.10 FTIR spectra of silica (a) and PCT-coated silica (b) particles, and the difference spectrum (c)

4.2.2 Morphology (SEM)

Scanning electron microscope (SEM) technique is applied to observe surface morphology of PCT-coated and uncoated silica particles. SEM images of silica and PCT-coated silica particles are compared in Figure 4.11. The size of the PCT-coated silica are smaller than the uncoated silica particles, and processes a rougher surface morphology (Figure 4.11a); while that of the surface of uncoated silica particles are smooth and has higher size uniformity. It is likely that the dispersion of silica during its formation step in PCT polymeric surfactant leads to the formation of surface roughness and the size reduction. The result is clearly observed in Figure 4.11. In addition, PCT can also decrease an agglomeration of silica particles by coating on their surface. It is expect that PCT may play some important roles in enhancing compatibility with the *l*-PLLA matrix. This will be examined in their composite materials.

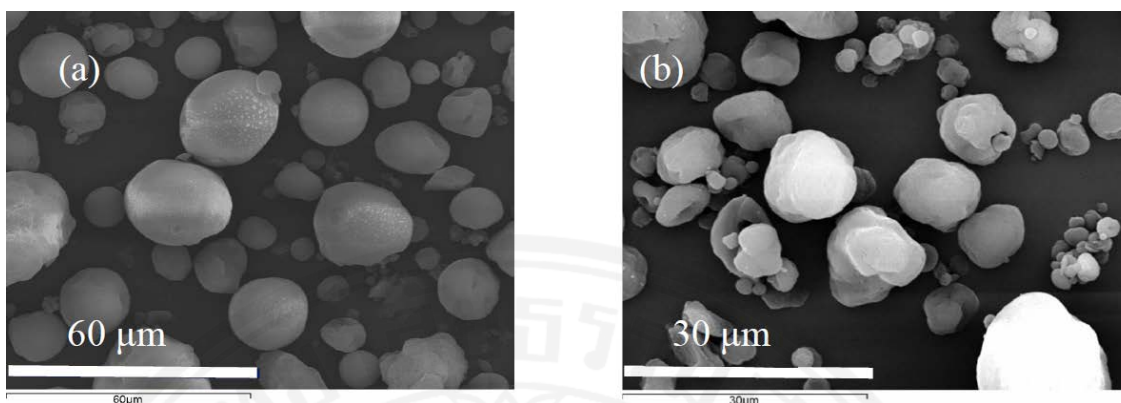


Figure 4.11 Scanning electron microscope of silica (a) and PCT-coated silica particles (b).

4.2.3 Particles size distribution

Two modes of particle size distribution are observed for both PCT-coated and uncoated particles, as described by S and M modes, reflecting their low uniformity particle size distribution. Data on size, surface area, and density of the silica and PCT-coated silica particles are summarized in Table 4.5. The size of the (S) and (M) groups are 16.2 ± 1.4 and 75.9 ± 1.3 μm , respectively. It is clearly seen that the particles size of PCT-coated silica process 2 times approximately smaller size than the uncoated particles, with the size 8.3 ± 1.5 (S) and 36.7 ± 1.4 μm (M), respectively. The smaller size of the PCT-coated silica particles is like an effect from the addition of PCT polymeric surfactant can reduce the particle size by breaking interaction between the silica structures within agglomerates. Surface area and density of the particles are also examining (Table 4.5). The surface area of PCT the coated particles are about 4 times larger than uncoated counterparts, which are 63.5 and 273.3 m^2/g , respectively. The larger surface area of the PCT-coated silica is perhaps due to the effect from their smaller size and the formation of rough layer of the polymer surfactant coated on the particle's surface. This agrees with the observed in SEM images. In addition, the coating of PCT on silica particle leads to a reduction in average density of the particles from 2.34 to 2.22 g/cm^3 to the presence of the lower density polymeric coating component.

Table 4. 5 particle size and size distribution, surface area, and density of silica and PCT-coated silica particles.

Sample	Average size (μm)		Surface area (m^2/g)	Density (g/cm^3)
	(s)	(M)		
	Silica	16.2 \pm 1.4	75.9 \pm 1.3	63.5
PCT-coated silica	8.3 \pm 1.5	36.7 \pm 1.4	273.3	2.22

4.2.4 Mechanical property (UTM)

The stress-strain behavior of *l*-PLLA and the composite materials of *l*-PLLA/ PCT-coated silica particles at 1.0 %wt. content of particles are examine. As shown in Figure 4.12, all samples are characterized as brittle materials with low percentage elongation, which is typical for composites containing particulate fillers.

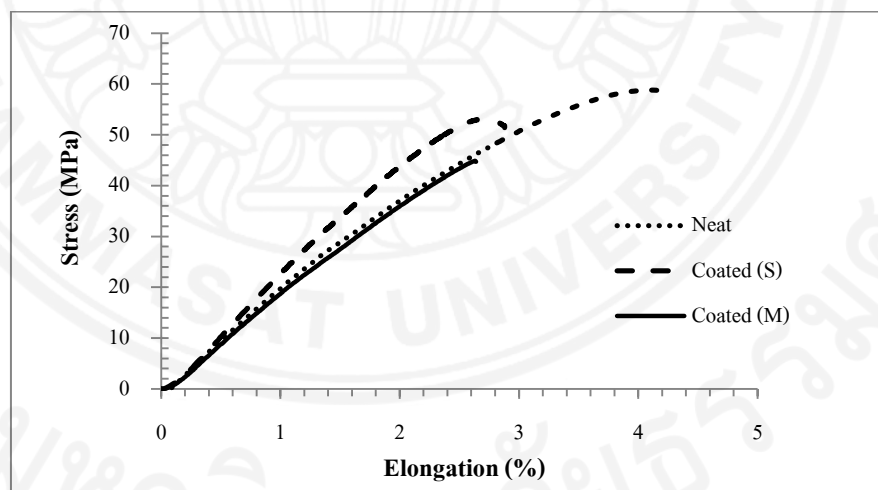


Figure 4.12 Stress-strain behaviors of *l*-PLLA and composite containing *l*-PLLA/ PCT-coated silica particles at 1.0 %wt. content.

As one of the important factors that affect the tensile property of *l*-PLLA/silica composites is the size of the particles, effects of silica particles size and their compositions on tensile strength, modulus, and elongation at break of the composites are examined. All tensile results of *l*-PLLA and *l*-PLLA/PCT-coated silica composite films are summarized in Table 4.6. The results show that tensile strength and elongation at break of both composites samples drastically drop when the silica particles are introduced into the *l*-PLLA matrix, as particulate filler cannot improve these properties of the materials, unlike fiber fillers. In contrast, modulus of the samples slightly increases with the addition of silica particles, due to the contribution from the more-rigid inorganic particles. In composite system, fillers are the components that carry the applied load which is transferred from the matrix during the tensile test, if the interfacial interactions between particles and the matrix are strong enough. There are many factors affecting tensile properties of polymer-inorganic composites, such as surface interaction, particles size and fillers distribution. Both chemical property and particle size of fillers have strong effect on their interfacial interaction in polymer composites. The fillers that have similar polarity and reactive functional groups with the polymer matrix may possess high reinforcement efficiency. However, functional groups located on fillers surface can induce agglomeration of these particles, therefore surface modification for some fillers are necessary for the preparation of polymer composites. The results show that *l*-PLLA/PCT-coated silica (S) composite films have higher tensile strength and elongation at break than the *l*-PLLA/PCT-coated silica (M) films at all silica compositions. It is concluded that this is originated from the different in their particle's size. Tensile properties of *l*-PLLA/PCT-coated silica composites films with different PCT-coated silica particle sizes and contents are shown Figure 4.13.

Table 4.6 Tensile results of *l*-PLLA and *l*-PLLA/PCT coated silica composite films containing particles with different sizes and blend contents.

SiO₂ Size	SiO₂ contents (%wt)	Strength (Mpa)	Elongation at break (%)	Modulus (Mpa)	Break energy (MJ/m²)
Silica (S)	0	59.9±1.7	4.1±0.4	2235±77	1490346
	0.5	52.7±1.2	3.07±0.3	2448±14	180232
	1	52.6±0.9	2.9±0.2	2455±73	742258
	1.5	56.7±0.4	3.0±0.2	2530±70	94626
Silica (M)	0	59.9±1.7	4.1±0.4	2235±77	1490346
	0.5	47.5±2.5	2.3±0.1	2302±74	742258
	1	43.8±6.8	2.2±0.1	2288±102	663965
	1.5	43.5±2.8	2.3±0.1	2337±143	658934

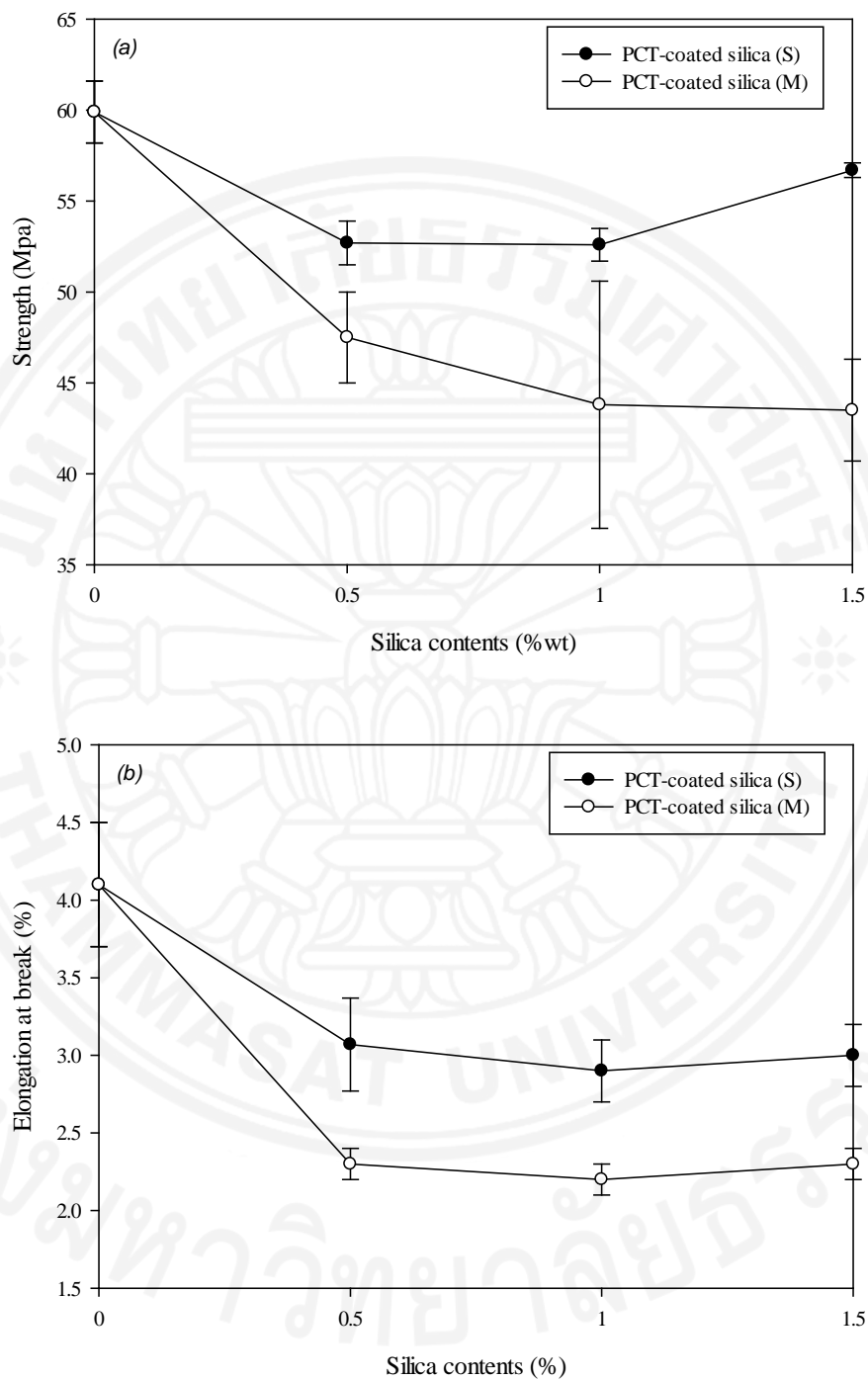


Figure 4.13 Tensile properties of *l*-PLLA/PCT-coated silica composite films with different PCT-coated silica particle sizes and contents (a) Tensile strength and (b) Elongation at break

4.2.5 Gas permeability

Recently, the applications of biodegradable polymers in the food packaging field are becoming interesting today. The target for using a polymer as packaging is to extend food shelf-life. Permeability is a crucial important factor for choosing a suitable material for specific food storage package applications. Generally, small molecules such as Oxygen (O_2), Carbon dioxide (CO_2) and water vapor (H_2O) can permeate through plastic films. Those molecules affect the shelf-life of food products. Oxygen Transmission Rate (OTR) and Carbon dioxide Transmission Rate (CO_2TR) are studied as key performance for plastic food packaging films, because these two gases play an important role as a preservative. Oxygen can speed up degradation rate of foods by oxidation reactions and corrosion. Carbon dioxide has the potential to reduce the degradation of some fresh foods, such as fruits and vegetables because it strongly affects the respiration rate of plant products by retarding the mechanism. Water Vapor Transmission Rate (WVTR) is also an important factor in plastic food packing films because some products require a permeation mechanism for dehydration, mean a low WVTR.

Specific permeation for specific gases is unique among different packaging materials, which depends on the characteristics of the food products. In order to study the effects of PCT-coated silica particles on gas permeability property of their composite films, Oxygen Transmission Rate (OTR), and Carbon dioxide Transmission Rate (CO_2TR) and Water Vapor Transmission Rate (WVTR) are examine. The results of neat *l*-PLLA and the composite films are compared in Table 4.7. All OTR, CO_2TR and WVTR values increase with an increase of the PCT-coated silica particle content and their particle size. This is likely a results from diffusion of gases through voids formed between particles and the *l*-PLLA matrix due to the incompatibility of the 2 components. In general, there are 3 steps of gas permeation through polymer films. The first step is dissolution and adsorption of gas molecules at the polymer surface. In the next step, the adsorbed (gases) molecules diffuse through the polymer and then desorb from the polymer, on the last step. A high degree of porosity and voids increased the permeability of gases through the polymer matrix by increasing both solubility and effective diffusion coefficients. If pores and voids are

present, the diffusion rates through these channels lead to an increase in the high permeation rate.

Table 4.7 OTR, CO₂TR, and WVTR of *l*-PLLA and *l*-PLLA/PCT-coated silica composite films

Sample	OTR (cm ³ ·mm/m ² ·day·atm)	CO₂TR (cm ³ ·mm/m ² ·day·atm)	WVTR (g/m ² ·day)
Neat	6	20	9
0.5 coated (M)	149	555	59
1.5 coated (S)	130	4450	-
1.5 coated (M)	891	13758	59

In addition, size, shape, chemical structures, and polarity of the diffused molecules also affect the gas permeation through the polymer matrix. The effect of polarity also observed on the WVTR of the composites films. The *l*-PLLA/ PCT-coated silica particles composites films show a higher WVTR, compared with *l*-PLLA films because of a high polarity in silica and the copolymer. More polarity from silica and the copolymer can increase the hydrophilicity of *l*-PLLA films, which allow more permeation of water molecules through the films. In this case, the diffusion coefficients of the films containing polar molecules are expected to increase due to the strong interactions between two polar molecules that induce structural transformations such as swelling or partial dissolution of the polymer matrix [18]. Gas selectivity behavior is also observed in the composites. The CO₂TR is roughly 4 times higher than that of OTR. Those results are from a higher affinity towards acidic CO₂ gas from amine groups present in chitosan units of PCT copolymer, compared to the natural O₂ molecules. For polymer composites, the absorption can be either increased or decreased depending on the relative solubility of the molecule in the matrix and filler. In this case, a high CO₂TR rate was obtained because of an increase of CO₂ solubility that strongly interact with the surfaces of PCT. CO₂ has an affinity toward the surface of PCT, coated with silica particles due to its acidity, which increases in the interface between the fillers, providing more absorption sites for the molecules, leading to an increase of solubility and absorption.

Chapter 5

Conclusions and Recommendations

5.1 Conclusions

Part 1 Preparation and characterization of hyper-branched PLLA (*hb*PLLAs) and *l*-PLLA/ *hb*PLLAs blend films

*hb*PLLAs have been successfully synthesized by using PEI as a macro initiator employing bulk polymerization of LLA. The arm's length of the *hb*PLLAs copolymer can be controlled by adjusting the feed ratios of PEI to LLA. Blended films between *l*-PLLA and the resulting *hb*PLLAs have been prepared and their properties were investigated. Improvements in the blends properties were achieved. The LLA arm's lengths of *hb*PLLA and the blend compositions have strongly effect on thermal, mechanical and rheological property of *l*-PLLA/*hb*PLLAs blends.

Part 2 Preparation and characterization of PCT-coated silica particles and *l*-PLLA/ PCT-coated silica composite films

PCT-coated silica composite films have been successfully synthesized in a single step process from rice hush ash. The coated particles were employed in a preparation of biocomposite materials. The *l*-PLLA/PCT-coated silica composites films show significant improvement in tensile modulus at 1.5%wt of the PCT-coated silica contents. Tunable gas permeability and selectivity of the composite films are achieved in *l*-PLLA/PCT-coated silica composites films. The materials are suitable for use as active packaging materials, which can be degraded after use.

5.2 Recommendations

1. Thermal, Mechanical, and rheological properties of *l*-PLLA/*hb*PLLAs blends can further optimize for specific applications by varying the branched structured composition.

2. Mechanical properties of *l*-PLLA/ *hb*PLLAs blends can further improve by blending or compositing them with other materials.

3. The particle size and distribution of PCT-coated silica particles can further optimize by adjusting the flow rate of CO₂ during the particle formation step in sol-gel process and concentration of polymeric surfactant and NaOH solution.

References

- [1] W. Zheng, J. Li, and Y. F. Zheng, "Preparation of poly(l-lactide) and its application in bioelectrochemistry," *Journal of Electroanalytical Chemistry*, vol. 621, pp. 69-74, 9/1/ 2008.
- [2] T. Ouchi, S. Ichimura, and Y. Ohya, "Synthesis of branched poly(lactide) using polyglycidol and thermal, mechanical properties of its solution-cast film," *Polymer*, vol. 47, pp. 429-434, 1/3/ 2006.
- [3] L. S. Nair and C. T. Laurencin, "Biodegradable polymers as biomaterials," *Progress in Polymer Science*, vol. 32, pp. 762-798, 8// 2007.
- [4] J.-M. Raquez, Y. Habibi, M. Murariu, and P. Dubois, "Polylactide (PLA)-based nanocomposites," *Progress in Polymer Science*.
- [5] J.-W. Rhim, S.-I. Hong, and C.-S. Ha, "Tensile, water vapor barrier and antimicrobial properties of PLA/nanoclay composite films," *LWT - Food Science and Technology*, vol. 42, pp. 612-617, 3// 2009.
- [6] M. Imanaka, Y. Takeuchi, Y. Nakamura, A. Nishimura, and T. Iida, "Fracture toughness of spherical silica-filled epoxy adhesives," *International Journal of Adhesion and Adhesives*, vol. 21, pp. 389-396, // 2001.
- [7] L. Urbanczyk, F. Ngoundjo, M. Alexandre, C. Jérôme, C. Detrembleur, and C. Calberg, "Synthesis of polylactide/clay nanocomposites by in situ intercalative polymerization in supercritical carbon dioxide," *European Polymer Journal*, vol. 45, pp. 643-648, 3// 2009.
- [8] N. Najafi, M. C. Heuzey, P. J. Carreau, and P. M. Wood-Adams, "Control of thermal degradation of polylactide (PLA)-clay nanocomposites using chain extenders," *Polymer Degradation and Stability*, vol. 97, pp. 554-565, 4// 2012.
- [9] K. Pongtanayut, C. Thongpin, and O. Santawitee, "The Effect of Rubber on Morphology, Thermal Properties and Mechanical Properties of PLA/NR and PLA/ENR Blends," *Energy Procedia*, vol. 34, pp. 888-897, // 2013.
- [10] R.-X. Zhao, L. Li, B. Wang, W.-W. Yang, Y. Chen, X.-H. He, *et al.*, "Aliphatic tertiary amine mediated synthesis of highly branched polylactide copolymers," *Polymer*, vol. 53, pp. 719-727, 2/2/ 2012.
- [11] C.-X. Zhang, B. Wang, Y. Chen, F. Cheng, and S.-C. Jiang, "Amphiphilic multiarm star polylactide with hyperbranched polyethylenimine as core: A systematic reinvestigation," *Polymer*, vol. 53, pp. 3900-3909, 8/17/ 2012.
- [12] A. Petchsuk, S. Buchatip, W. Supmak, M. Opaprakasit, and P. Opaprakasit, "Preparation and properties of multi-branched poly(D-lactide) derived from

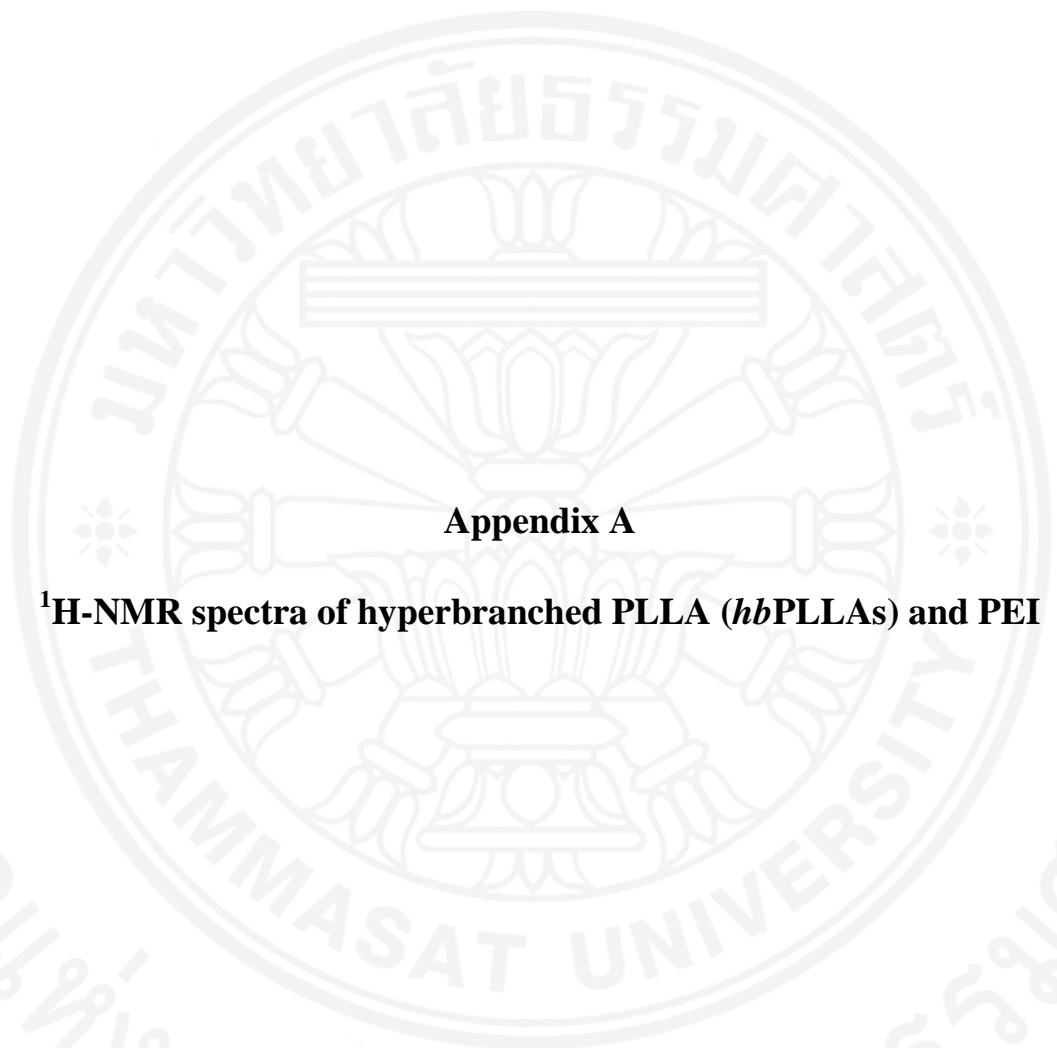
- polyglycidol and its stereocomplex blends," *Express Polymer Letters*, vol. 8, pp. 779-789, 2014.
- [13] A. M. Fischer, R. Thiermann, M. Maskos, and H. Frey, "One-pot synthesis of poly(l-lactide) multi-arm star copolymers based on a polyester polyol macroinitiator," *Polymer*, vol. 54, pp. 1993-2000, 4/3/ 2013.
- [14] M.-A. Paul, M. Alexandre, P. Degée, C. Henrist, A. Rulmont, and P. Dubois, "New nanocomposite materials based on plasticized poly(l-lactide) and organo-modified montmorillonites: thermal and morphological study," *Polymer*, vol. 44, pp. 443-450, 1// 2003.
- [15] S. Sinha Ray, K. Yamada, M. Okamoto, Y. Fujimoto, A. Ogami, and K. Ueda, "New polylactide/layered silicate nanocomposites. 5. Designing of materials with desired properties," *Polymer*, vol. 44, pp. 6633-6646, 10// 2003.
- [16] H. Balakrishnan, A. Hassan, M. Imran, and M. U. Wahit, "Toughening of polylactic acid nanocomposites: A short review," *Polymer-Plastics Technology and Engineering*, vol. 51, pp. 175-192, 2012.
- [17] R. Datta and M. Henry, "Lactic acid: recent advances in products, processes and technologies — a review," *Journal of Chemical Technology & Biotechnology*, vol. 81, pp. 1119-1129, 2006.
- [18] L. Yu, K. Dean, and L. Li, "Polymer blends and composites from renewable resources," *Progress in polymer science*, vol. 31, pp. 576-602, 2006.
- [19] B. Li, F.-X. Dong, X.-L. Wang, J. Yang, D.-Y. Wang, and Y.-Z. Wang, "Organically modified rectorite toughened poly(lactic acid): Nanostructures, crystallization and mechanical properties," *European Polymer Journal*, vol. 45, pp. 2996-3003, 11// 2009.
- [20] S. Yan, J. Yin, Y. Yang, Z. Dai, J. Ma, and X. Chen, "Surface-grafted silica linked with l-lactic acid oligomer: A novel nanofiller to improve the performance of biodegradable poly(l-lactide)," *Polymer*, vol. 48, pp. 1688-1694, 3/8/ 2007.
- [21] T. Ribeiro, C. Baleizão, and J. Farinha, "Functional Films from Silica/Polymer Nanoparticles," *Materials*, vol. 7, p. 3881, 2014.
- [22] U. Kalapathy, A. Proctor, and J. Shultz, "A simple method for production of pure silica from rice hull ash," *Bioresource Technology*, vol. 73, pp. 257-262, 7// 2000.
- [23] M. Mohamed Jaffer Sadiq and A. Samson Nesaraj, "Development of NiO-Co3O4 nano-ceramic composite materials as novel photocatalysts to degrade

- organic contaminants present in water," *International Journal of Environmental Research*, vol. 8, pp. 1171-1184, 2014.
- [24] Y. Fan, H. Nishida, Y. Shirai, Y. Tokiwa, and T. Endo, "Thermal degradation behaviour of poly(lactic acid) stereocomplex," *Polymer Degradation and Stability*, vol. 86, pp. 197-208, 11// 2004.
- [25] J. Geschwind, S. Rathi, C. Tonhauser, M. Schömer, S. L. Hsu, E. B. Coughlin, *et al.*, "Stereocomplex Formation in Polylactide Multiarm Stars and Comb Copolymers with Linear and Hyperbranched Multifunctional PEG," *Macromolecular Chemistry and Physics*, vol. 214, pp. 1434-1444, 2013.
- [26] S. R. Andersson, M. Hakkarainen, and A.-C. Albertsson, "Stereocomplexation between PLA-like substituted oligomers and the influence on the hydrolytic degradation," *Polymer*, vol. 54, pp. 4105-4111, 7/19/ 2013.
- [27] K. Madhavan Nampoothiri, N. R. Nair, and R. P. John, "An overview of the recent developments in polylactide (PLA) research," *Bioresource Technology*, vol. 101, pp. 8493-8501, 11// 2010.
- [28] S. Yan, J. Yin, J. Yang, and X. Chen, "Structural characteristics and thermal properties of plasticized poly(l-lactide)-silica nanocomposites synthesized by sol-gel method," *Materials Letters*, vol. 61, pp. 2683-2686, 5// 2007.
- [29] J.-C. Lin, "Investigation of impact behavior of various silica-reinforced polymeric matrix nanocomposites," *Composite Structures*, vol. 84, pp. 125-131, 7// 2008.
- [30] G. Bang and S. W. Kim, "Biodegradable poly(lactic acid)-based hybrid coating materials for food packaging films with gas barrier properties," *Journal of Industrial and Engineering Chemistry*, vol. 18, pp. 1063-1068, 5/25/ 2012.
- [31] J.-W. Rhim, "Effect of clay contents on mechanical and water vapor barrier properties of agar-based nanocomposite films," *Carbohydrate Polymers*, vol. 86, pp. 691-699, 8/15/ 2011.
- [32] C. Thammawong, P. Sreearunothai, A. Petchsuk, P. Tangboriboonrat, N. Pimpha, and P. Opaprakasit, "Preparation and characterizations of naproxen-loaded magnetic nanoparticles coated with PLA-g-chitosan copolymer," *Journal of Nanoparticle Research*, vol. 14, pp. 1-12, 2012/07/25 2012.
- [33] S. Peleshanko and V. V. Tsukruk, "The architectures and surface behavior of highly branched molecules," *Progress in Polymer Science*, vol. 33, pp. 523-580, 5// 2008.

- [34] M. Mihai, M. A. Huneault, and B. D. Favis, "Rheology and extrusion foaming of chain-branched poly(lactic acid)," *Polymer Engineering & Science*, vol. 50, pp. 629-642, 2010.
- [35] J. Matusik, E. Stodolak, and K. Bahranowski, "Synthesis of polylactide/clay composites using structurally different kaolinites and kaolinite nanotubes," *Applied Clay Science*, vol. 51, pp. 102-109, 1// 2011.
- [36] J.-W. Rhim, H.-M. Park, and C.-S. Ha, "Bio-nanocomposites for food packaging applications," *Progress in Polymer Science*.
- [37] J. Jiao, X. Sun, and T. J. Pinnavaia, "Mesostructured silica for the reinforcement and toughening of rubbery and glassy epoxy polymers," *Polymer*, vol. 50, pp. 983-989, 2/9/ 2009.
- [38] A. Pr  b  , P. Alcouffe, P. Cassagnau, and J. F. G  rard, "In situ polymerization of l-Lactide in the presence of fumed silica," *Materials Chemistry and Physics*, vol. 124, pp. 399-405, 11/1/ 2010.
- [39] C. Thammawong, P. Sreearunothai, A. Petchsuk, P. Tangboriboonrat, N. Pimpha, and P. Opaprakasit, "Preparation and characterizations of naproxen-loaded magnetic nanoparticles coated with PLA-g-chitosan copolymer," *Journal of Nanoparticle Research*, vol. 14, 2012.
- [40] T. H. Nguyen, P. Tangboriboonrat, N. Rattanasom, A. Petchsuk, M. Opaprakasit, C. Thammawong, *et al.*, "Polylactic acid/ethylene glycol triblock copolymer as novel crosslinker for epoxidized natural rubber," *Journal of Applied Polymer Science*, vol. 124, pp. 164-174, 2012

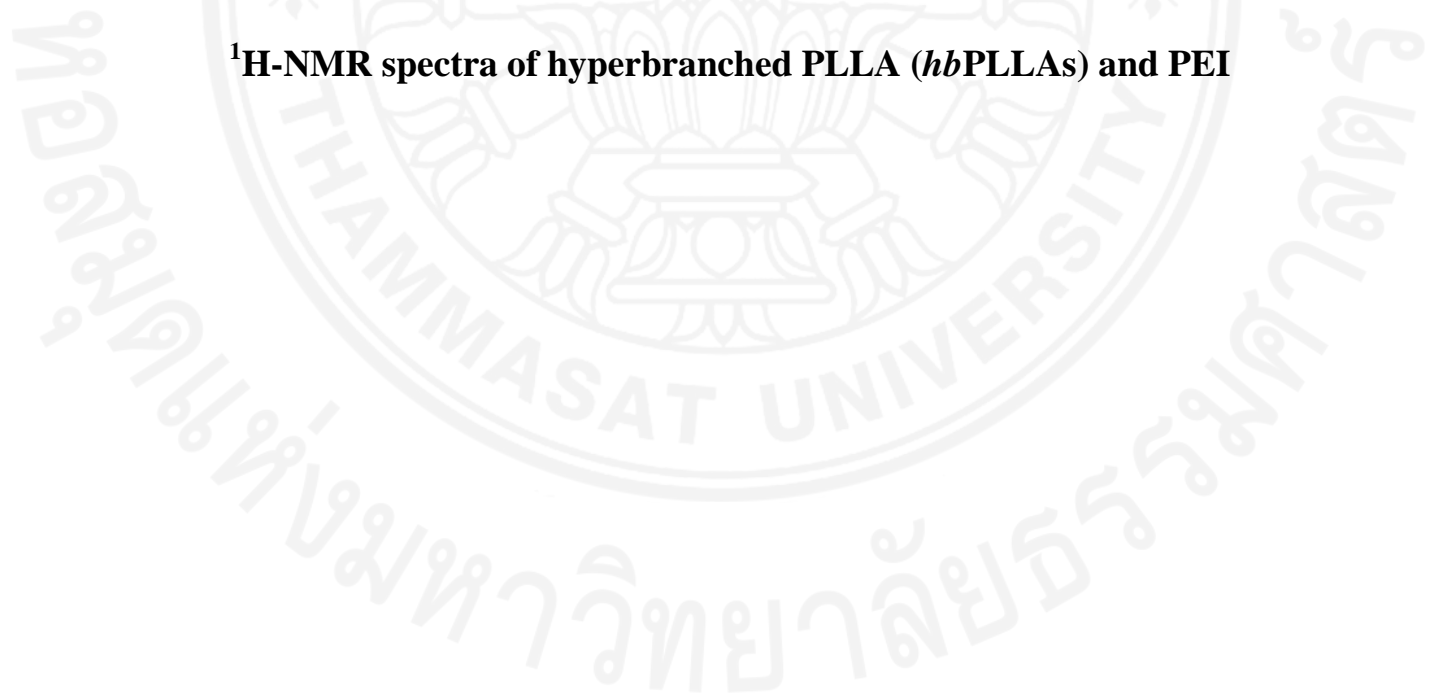
Appendices

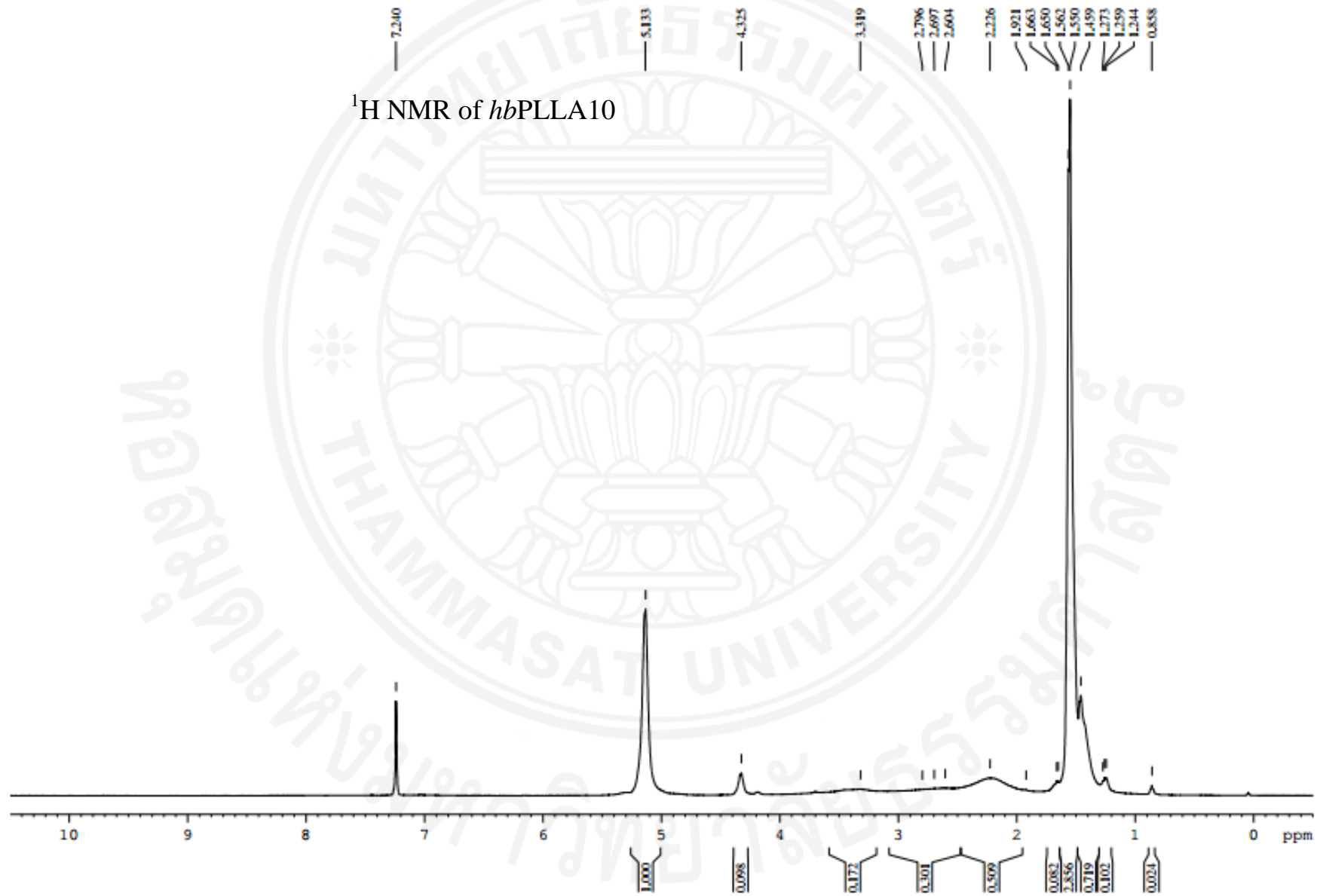


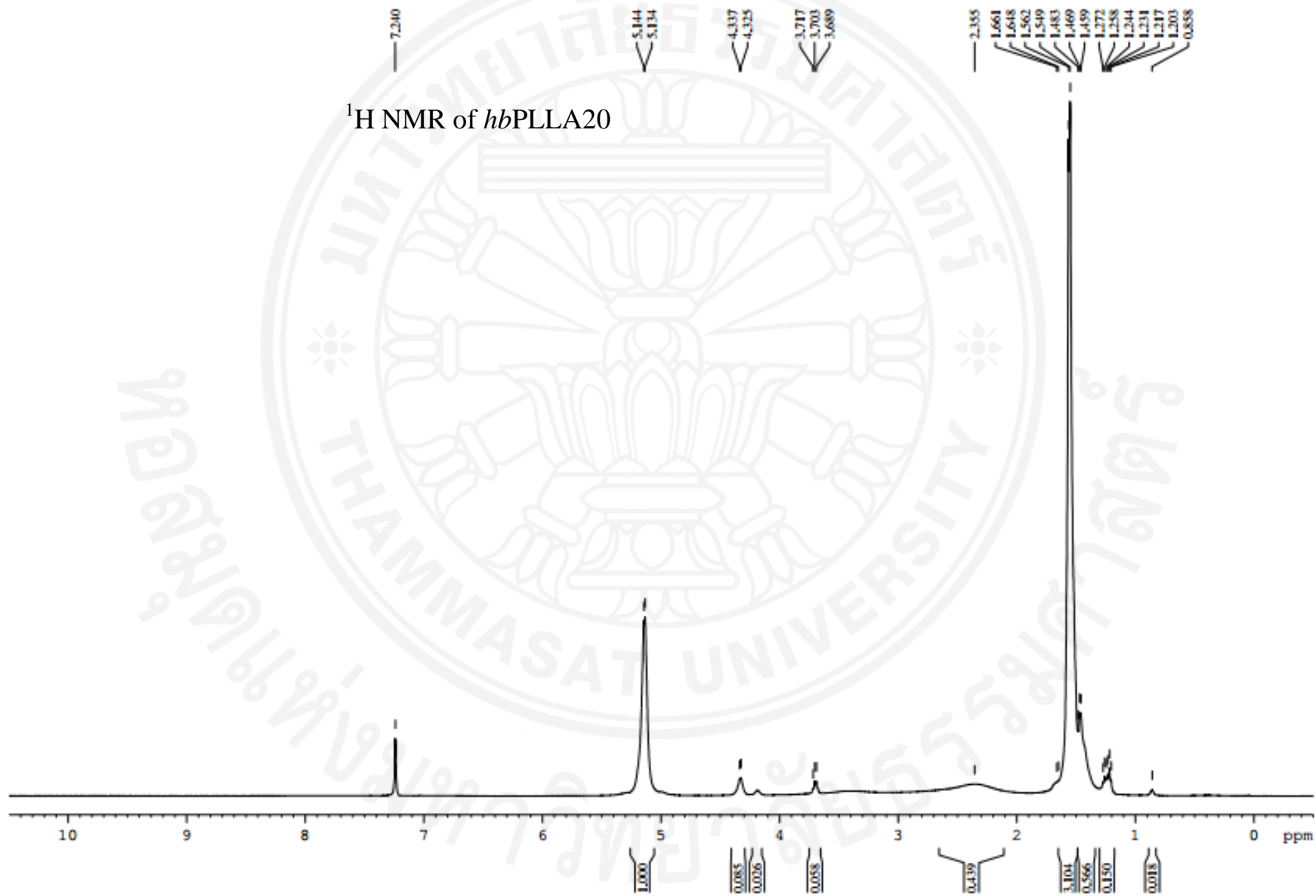


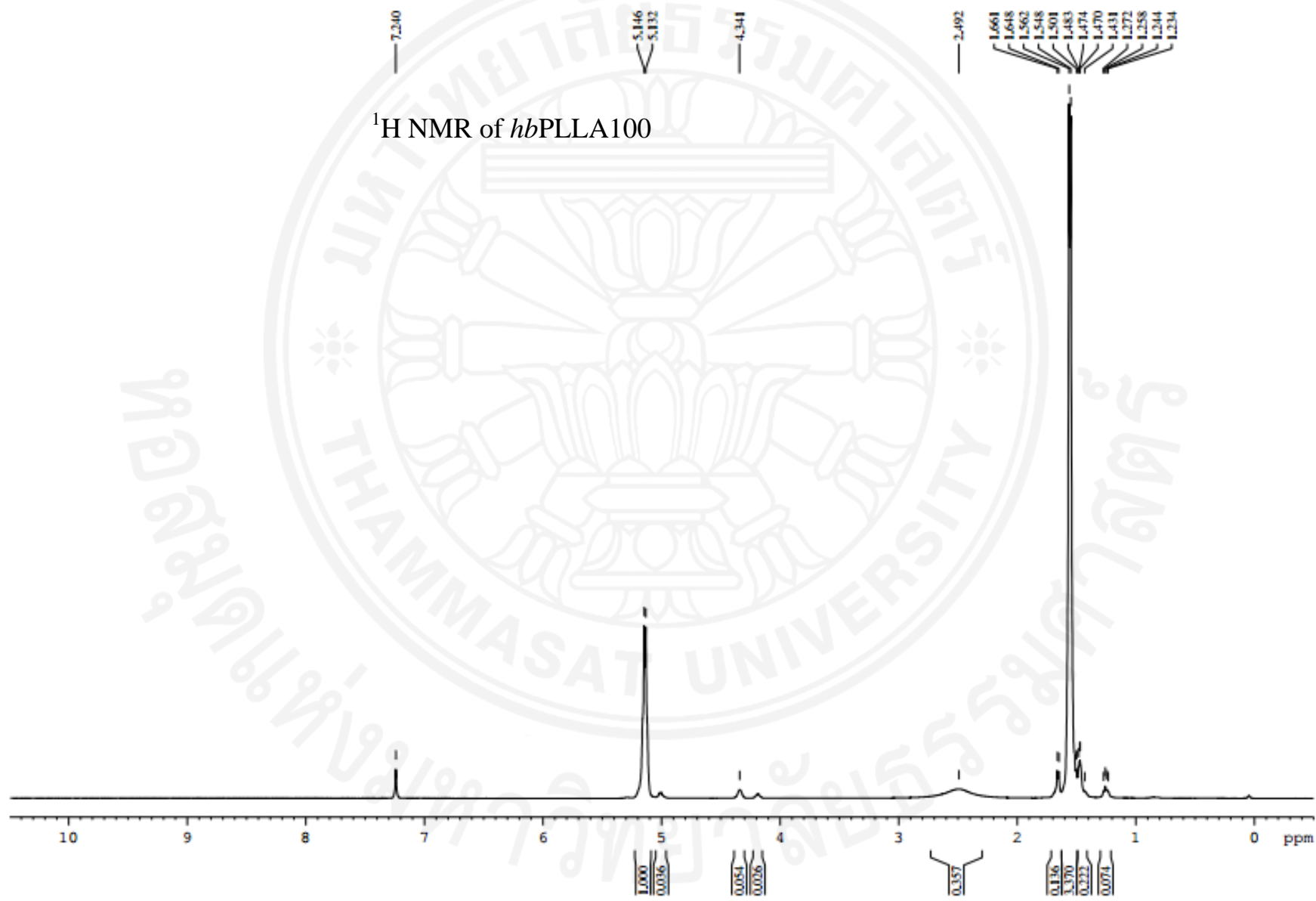
Appendix A

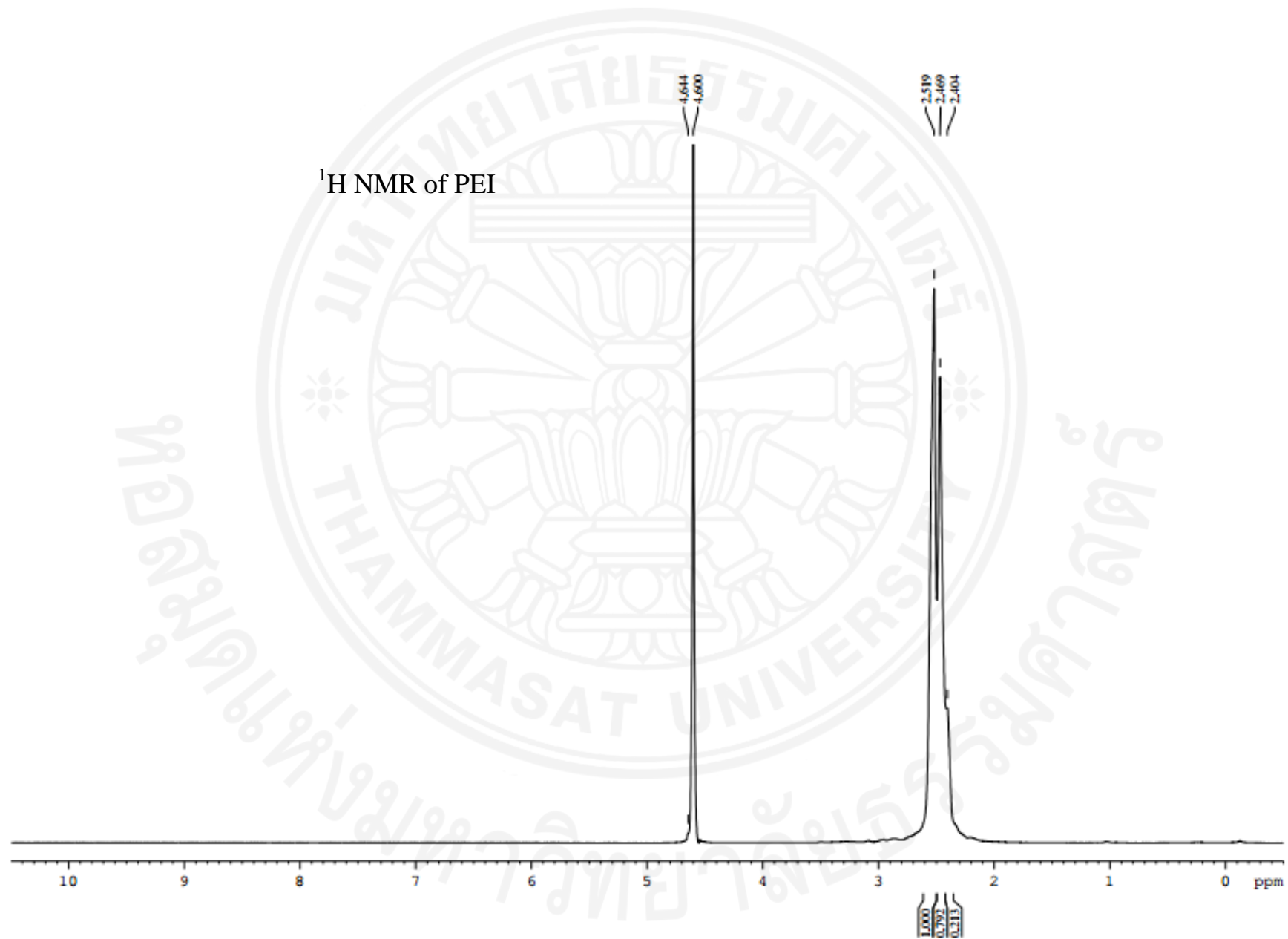
¹H-NMR spectra of hyperbranched PLLA (*hb*PLLAs) and PEI











Appendix B

Publication

